
Design & Implementation of
digital channel selection filters
for a combined BlueTooth and
HiperLAN/2 receiver

Master's Thesis

Lars van Mourik

University of Twente

University of Twente
Department of Electrical Engineering
Chair of Signals & Systems
Enschede, The Netherlands

Supervisors: Prof. Dr. Ir. C.H. Slump
Ir. F.W. Hoeksema
Ir. R. Schiphorst
Ir. V.J. Arkesteijn
Date: 22 August 2002
Period: January 2002 - August 2002
Report Code: SAS033N02

Abstract

In the context of a Software Defined Radio (SDR) receiver, digital channel selection filters were researched for Bluetooth and HiperLAN/2 signals. The goal was to derive the specifications and find suitable implementations, as well as building a simulation model. This model includes the digital channel selection system for both Bluetooth and HiperLAN/2 with analog front-end and demodulators. For HiperLAN/2 the proposed filter system is based on poly-phase low-pass FIR filters and theoretical specifications. Due to late availability of a demodulator, this system was not further researched. For Bluetooth, The *real* and The *complex* filter systems were researched including the feasibility of using (non linear phase) IIR filters. The *real* design was implemented and improved and is proposed as the optimal solution for the current requirements with respect to the derived performance figure. The incoming quadrature signals are low-pass filtered by a pair of (real) FIR filters, implemented in polyphase. Then, they are converted to a bandpass signal by using a FIR Hilbert transformer and adder. Changing the sign bit of the adder is the first stage of channel selection. Then, the signals are band-pass filtering by a *variable* 4th order Chebyshev Type II IIR filter. The filter is variable in the sense that filter coefficients must be updated every time the Bluetooth signal hops to another frequency. Then the filtered signal is mixed to the required frequency for demodulation. After a second band-pass filter (6th order Butterworth IIR filter) the signal is decimated again and ready for demodulation. The choice for IIR filters was made to reduce filter operations. A FIR-only design was also proposed and can be used in case IIR filters are not suitable for implementation. Both systems meet BER requirements as specified in the Bluetooth documentation.

Contents

Contents	1
1 Introduction	3
1.1 Background	3
1.2 Thesis objectives	3
1.3 Thesis structure	4
2 Channel selection: initial requirements	5
2.1 Introduction	5
2.2 Analog front-end	5
2.3 Digital channel selection	7
2.4 Filter requirements	8
2.5 Demodulator imposed requirements	10
2.6 Recapitulation of known parameters	11
3 Channel selection - detailed requirements	13
3.1 Introduction	13
3.2 Analog front-end	13
3.3 Requirements imposed by the demodulator	16
3.4 Channel selection system	17
3.5 Conclusions	19
4 Filter and Decimate	21
4.1 Introduction	21
4.1.1 Design parameters	21
4.1.2 Filter performance	22
4.2 FIR	25
4.2.1 Least squared error	25
4.2.2 Windowing	25
4.2.3 Uniform approximation	25
4.2.4 Influence of Δf and δ_p on N	26
4.2.5 Multi-rate	27
4.2.6 Polyphase filters	33
4.2.7 Complex filters	36
4.3 CIC	36
4.4 IIR	39
4.4.1 Bilinear transform	39
4.4.2 Group delay	39
4.4.3 Filter types	39
4.4.4 Demodulator sensitivity tests	41
4.4.5 Conclusions	45

5	Digital Mixer	46
5.1	Introduction	46
5.2	Real Mixer	46
5.3	Hilbert-mixer	46
5.4	Required mixer frequencies	46
5.5	Conclusions	47
6	System	49
6.1	Introduction	49
6.2	Test environment and parameters	49
6.2.1	BER tests	49
6.3	ASAP system 1	51
6.3.1	Introduction	51
6.3.2	Hilbert transformer (Hb) design	52
6.3.3	Post mixer filter (BPF2) design	52
6.3.4	Spectral analysis of the systems signals	53
6.3.5	Eye diagrams	55
6.3.6	BER calculations	57
6.3.7	ASAP system 1 specification	57
6.4	ASAP system 2	58
6.4.1	Introduction	58
6.4.2	Moving the Hilbert bottle-neck	58
6.4.3	Reduce aliasing, improve BPF1/BPF2 cooperation	59
6.4.4	BPF1/BPF2 filter re-design	59
6.4.5	Sensitivities and trade-offs	60
6.4.6	ASAP system 2 specifications	60
6.5	ALAP system	61
6.6	Conclusions	61
7	Conclusions and Recommendations	62
7.1	Conclusions (Summary)	62
7.2	Recommendations	63
A	Quadrature signals	64
A.1	In-phase and Quadrature signals	64
A.2	Quadrature down conversion of signal chunks	64
B	The Hilbert transform	66
B.1	Practical usage for channel selection	67
B.2	Upper/lower sideband rejection	67
C	Noble identities	70
	Bibliography	71

Introduction

1.1 Background

This thesis was done in the context of a Software Defined Radio (SDR) project. A SDR is a software implementation of a mobile user terminal able to dynamically adapt to the radio environment in which it is located. For a manufacturer, a single design is sufficient for the whole world and consumers can use their mobile terminals in every country. Because of the analog nature of the air interface, a software radio will always have an analog front end. In an ideal software radio, the analog-to-digital and digital-to-analog (A/D-D/A) converters are positioned directly after the antenna. Such an implementation is not feasible due to the power that such device would consume and other physical limitations. It is therefore a challenge to design a system that preserves most properties of the ideal software radio while being realizable with current-day technology. In figure 1.1 the different functions of a radio receiver are shown: an analog front-end, followed by digital channel selection and a demodulator. The analog front-end receives RF signals and converts them to a suitable lower frequency. After AD conversion, channels are selected and demodulated in the digital domain. Generally spoken, the channel selection function is to be realized with filters, down-converters and mixers.

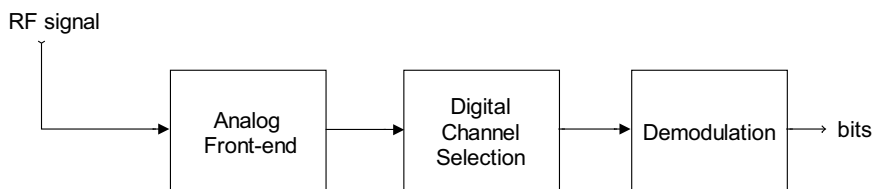


Figure 1.1: Channel selection function in the SDR receiver

1.2 Thesis objectives

This document will focus on the digital channel selection of the mobile receiver terminal. Research on this subject includes the derivation of filter specifications, given the channel selection requirements of Bluetooth and HiperLAN/2. Based on these specifications a literature study is to be done on digital filters to find suitable designs methods. Then, a working model of the digital part of the software defined radio must be built including the contributions of other project members. With this

model, simulations of selected filter designs are done to discover the design space and optimize the system with respect to power consumption.

1.3 Thesis structure

At the start of this assignment, a lot of design options for the entire receiver were still left unanswered due to the state the project was in at that moment. Based on an initial study into the Bluetooth and HiperLAN/2 specifications a general context was created which was used as a starting point for the design process. This context is given in chapter 2, where an effort was made to cope with the uncertainties by defining scenario's and configurations. As the project progressed, more information became available on the surrounding system components. Based on this information, new insights and research area's were uncovered and designs choices were rethought. The new and more detailed context is given in chapter 3. Based on the derived specifications, chapter 4 researches digital filters and suitable implementations. Chapter 5 gives an overview of digital mixing, which is also required for the channel selection. Then, chapter 6 discusses channel selection models that were designed and compares their performance with respect to bit errors and filter operations. Design parameters, constraints, issues and trade-offs of the proposed systems are discussed and recommendations for future work are given.

2

Channel selection: initial requirements

2.1 Introduction

The channel selection system under research in this document is part of a larger system, namely the receiver. Referring to [7], it is part of the subsystem in between the Antenna Reference Point and the Channel Reference Point. Due to hardware constraints, both analog and digital processing is needed for channel selection. This

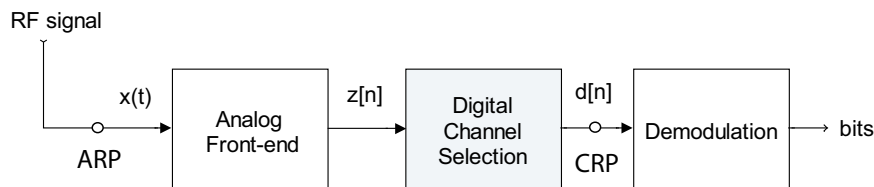


Figure 2.1: Channel selection function in the receiver

document describes the design of the digital part of the channel selection subsystem (see figure 2.1). The combined Bluetooth and HiperLAN/2 receiver terminal poses a list of demands on the signal conditioning for a well-defined signal configuration to achieve a certain BER. The subsystem under design is the interface between the analog front-end and the demodulator, both introducing constraints. Initial constraints, based on the specifications will be discussed in this chapter. For each of the three sub-blocks in figure 2.1 the known and unknown parameters will be listed. As the design of the receiver was an ongoing project more specific requirements became available at a later time. In *this chapter* it was assumed that the demodulator was not finished and that the exact output of the analog front-end is not specified. These specifications and resulting design choices for the digital channel selection system are added in chapter 3.

2.2 Analog front-end

Generally, the analog front-end will contain an amplifier, band-pass filter and mixer to convert the received signal to a suitable intermediate frequency or baseband. In this case, the received signal can be either a part of the Bluetooth or HiperLAN/2 spectrum. The Bluetooth spectrum resides in the 2.4 GHz band and the Hiper-

LAN/2 signals in the 5 GHz band. Initially, this part of the system will be seen as a black box, outputting 10 or 20 MHz chunks of "signal" at a low rate. This rate is defined by the Analog to Digital Converter (ADC), which is assumed to be a part of the analog front-end. The actual sampling rate f_{AD} and resolution of the AD conversion are not known yet, but for exploration purposes $f_{AD}=60, 80$ and 100 Mega samples per second (Ms/s) are assumed.

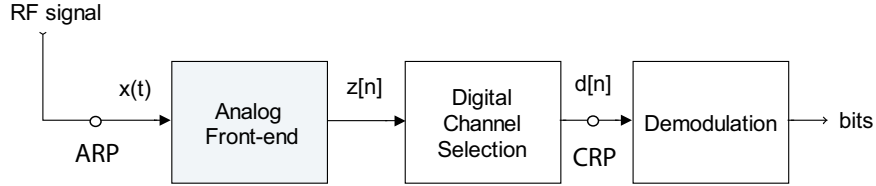


Figure 2.2: Analog front-end

Scenario's

For convenience of reference, the incoming (RF) signal is called $x(t)$ (refer to figure 2.2). The positive half of the spectrum of the signal is depicted in figure 2.2. Theoretically, the width of the spectrum outputted by the front-end is only bound by the sample frequency of the ADC (f_{AD}). Thus, the spectral location of the incoming Bluetooth or HiperLAN/2 signal chunks can be anywhere in between 0 and $f_{AD}/2$. In this region two fundamentally different locations can be identified, namely *baseband* and *IF*. *IF* is an **I**ntermediate **F**requency, and a distinction will be made between low and medium *IF*. This distinction is arbitrary and will be explained in section 2.5. With these distinctions, 3 scenario's will be discussed separately for HiperLAN/2 and Bluetooth in the following sections. In chapter 3 the alternatives presented will be pinned further, as more project-knowledge is available there. The output of the analog front-end (and thus the input of the digital channel selection subsystem) is called $z(n)$ (see also figure 2.2).

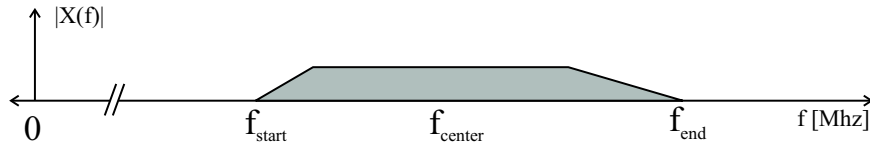


Figure 2.3: Spectrum of a signal chunk at RF

HiperLAN/2

In case HiperLAN/2 signals are received, the Fourier transform $X(f)$ of $x(t)$ is shown in figure 2.2. This spectrum represents one HiperLAN/2 channel that is frequency shifted from RF (≈ 5 GHz) to a much lower (intermediate) frequency. In figure 2.4, the shaded boxes represent the HiperLAN/2 spectra and the white boxes their negative mirrors. If the frequency of the local oscillator in the analog front-end is chosen to equal the center frequency of this channel (f_{center} in figure 2.2), the result (after low-pass filtering) is shown in figure 2.4(a). In this case, the analog front-end output is a complex (baseband) signal. If the local oscillator in the analog front-end has a frequency equal to f_{start} in figure 2.2, the result is shown in

figure 2.4(b). With a local oscillator frequency lower than f_{start} , the spectrum is located as in figure 2.4(c).

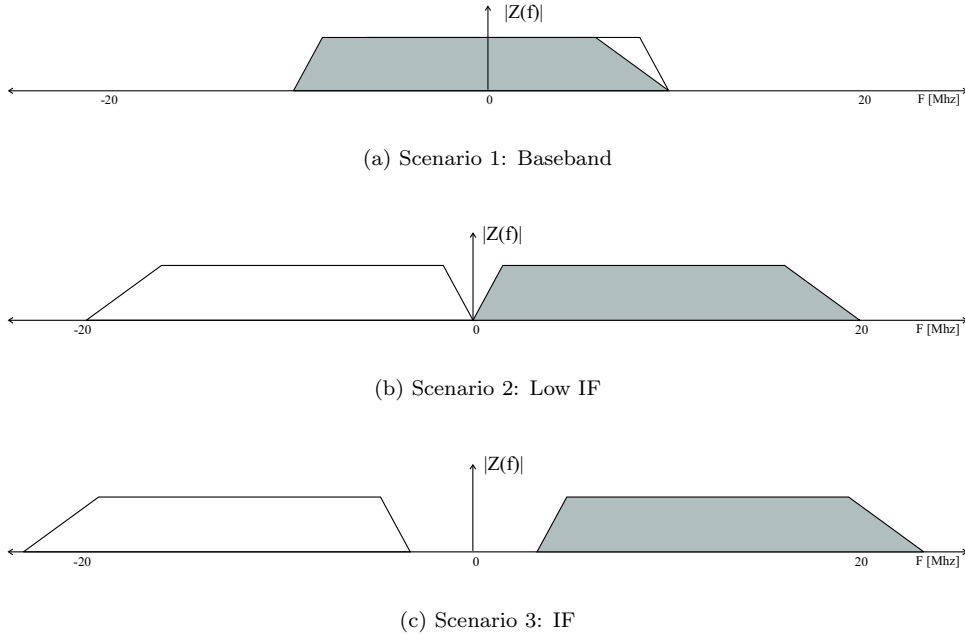


Figure 2.4: Analog front-end output spectra (HiperLAN/2): three scenario's

Bluetooth

For Bluetooth, the analog output scenario's are generally the same as for HiperLAN/2. But now, $X(f)$ in figure 2.2 represents 20 Bluetooth channels. In figure 2.5 this is depicted by the shaded boxes (representing the positive spectra) numbered 0–19. The white boxes are their corresponding negative spectra. The Bluetooth demodulator requires a band-pass signal (thus having an even spectrum). This means that in case of scenario 1, (the local oscillator in the analog front-end is equal to f_{center} in figure 2.2), the resulting baseband signals require additional processing to be converted to band-pass.

2.3 Digital channel selection

Attenuation by propagation, path loss, multi-path fading and adjacent channel interference are just few of the unwanted effects that reduce the desired signal quality. In addition, the receiver system itself adds noise to the signal. A common method of removing interference from a signal is filtering. For both Bluetooth and HiperLAN/2 worst case input scenario's are given in [11]. These will be the basis upon which the filters are designed. Note however that exact requirements with respect to certain filter characteristics are not known yet. Unknown parameters include: maximum allowable values for the so-called pass-band ripple, phase non-linearity and required attenuation in the transition bands. These transition bands are the bands "in between the channels" and defined as "don't care" bands in [11]. The demodulator performance reduction due to these effects should be more thoroughly researched or determined by for instance simulations. The Bluetooth modulation

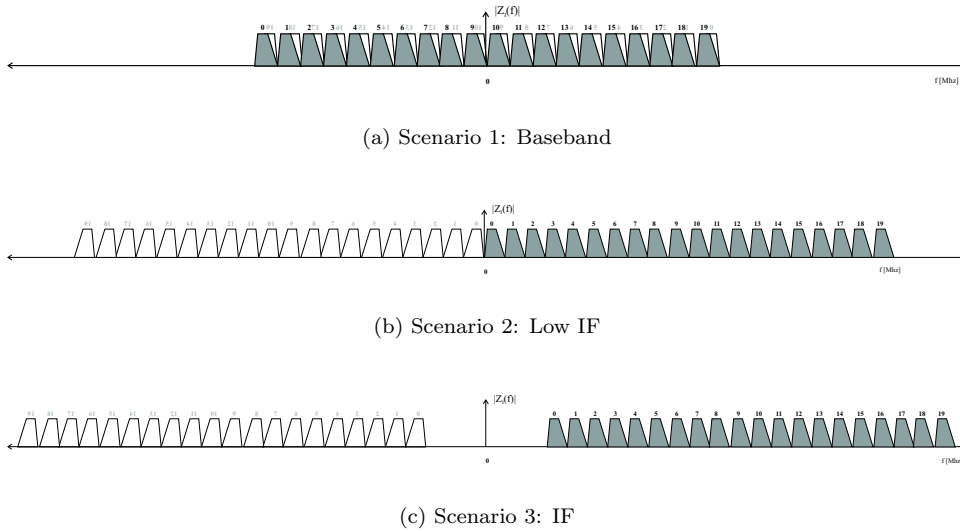


Figure 2.5: Analog front-end output spectra (Bluetooth): three scenario's

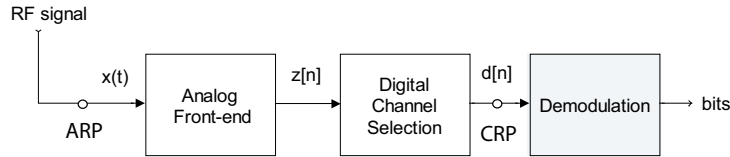


Figure 2.6: Demodulator

scheme is GFSK [23], whereby the transmitted bits are frequency modulated. It is therefore assumed that FIR filters are more suitable (than IIR) due to their exact linear phase response. HiperLAN/2 is modulated using OFDM which is also sensitive to phase distortions, resulting in inter carrier interference (ICI) [16].

2.4 Filter requirements

HiperLAN/2

For a HiperLAN/2 signal, the channel selection is assumed to be mainly done by the analog front end. The resulting spectrum may require some conditioning to achieve the specifications listed below. Depending on the final front-end architecture, one of the three scenario's below will be implemented. The filter specifications for a chunk centered at baseband are:

- Pass-band: 8.28125 MHz
- Transition band: 8.28125 - 11.71875 MHz
- Stop band: 11.71875 - 28.8125 MHz, minimum attenuation: 32 dB
- Transition band: 28.28125 - 31.71875 MHz
- Stop band: ≥ 31.71875 , minimum attenuation: 51 dB

A graphical representation of these is shown in figure 2.7 [11]. The three analog front-end output scenario's are depicted in figure 2.4.

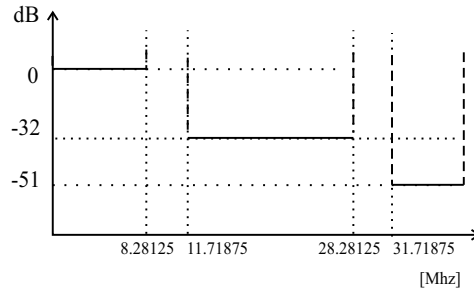


Figure 2.7: Low-pass filter requirements HiperLAN/2 [11]

Bluetooth

The signal chunk from the analog front-end contains 10 or 20 Bluetooth channels. This means that for each selected channel, there can be up to 19 interferers "polluting" the signal. The degree of interference for which the receiver must have adequate performance has been quantified in the Bluetooth specifications [23]. Four different cases of strong interference are given for which the receiver must achieve a maximum bit error rate (BER) of 0.1%. Filter specifications based on these tests were derived in [11], and specified for a Bluetooth signal, centered at baseband. The bandwidth of the signal holding 98% of it's power is 0.675MHz . With equally spaced channels, in between their 98% bandwidth is assumed to be a "don't care" region. The receiver must be able to sufficiently attenuate these strong interferers:

- Adjacent (1MHz) channel interferer: same strength
- Adjacent (2MHz) channel interferer: 30 dB stronger
- Adjacent ($\geq 3\text{MHz}$) channel interferer: 40 dB stronger

The fourth strong interference is in-band and 11 dB weaker than the wanted channel. From the adjacent channel tests, filter requirements were derived. Note that these requirements seem to imply that all interferers are present simultaneously, but this is not the case. Theoretically, three filter specification could have been made for each case of strong interference, but that would require the receiver to have real-time "knowledge" of the interference levels. Thus, a composite filter response is given for all interferers, and more relaxed specifications must be derived while conducting BER tests. The following (composite) filter requirements are derived for a wanted channel centered at baseband (see also figure 2.8):

- Pass-band: 0 - 0.34 MHz
- Transition band: 0.34 - 0.66 MHz
- Stop band: 0.66 - 1.34 MHz, minimum attenuation: 24 dB
- "Don't care" band: 1.34 - 1.66 MHz
- Stop band: 1.66 - 2.34 MHz, minimum attenuation: 54 dB
- "Don't care" band: 2.34 - 2.66 MHz
- Stop band: 2.66 - 3.34 MHz, minimum attenuation: 64 dB

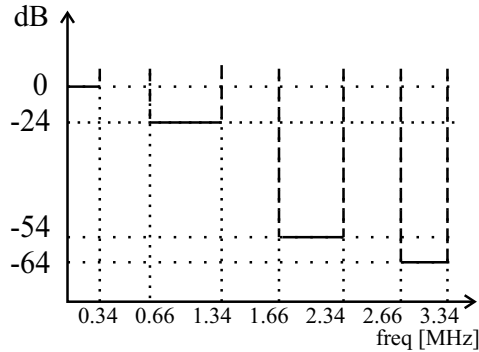


Figure 2.8: Low-pass filter requirements Bluetooth [11]

Note that the requirements given apply to the combined analog and digital filters between the ARP and CRP (refer to figure 2.6). However in [7] it is stated that after analog processing the given requirements are likely to remain valid for the digital filter system. This composite filter response assumes that the selected channel is at baseband. In practice, the selected channel can be anywhere in the frequency interval $-f_{AD}/2 \leq f_c \leq f_{AD}/2$, depending on the output scenario of the analog front-end. In addition, the selected channel will be frequency hopping¹². This generally leaves two options:

1. Derive a different set of filter specifications for each possible (spectral) location of the selected channel. The targeted filter response will then be a frequency shifted version of the spectrum depicted in figure 2.8.
2. Use a frequency translation method to "move" the selected channel to the (spectral) location specified by the filter

Further studies will be carried out to find a practical solution for this.

2.5 Demodulator imposed requirements

HiperLAN/2

The signal chunk provided by the analog front-end is already the input for its demodulator. The digital channel selection of the modulated sub-channels [11] is done in the HiperLAN/2 demodulator. This demodulator requires quadrature (baseband) inputs, thus for scenario 1 (refer to figure 2.4) low-pass filtering both I and Q paths suffices and no additional processing is necessary. The input rate of the demodulator is likely to be an integer multiple of the channel width, which is 20 MHz.

Bluetooth

Frequency translation

After filtering, the desired channel must be demodulated. Depending on the implementation of the demodulator, it may require the channel to be frequency translated

¹As stated in the Bluetooth specification [23], so the channel selection criteria "change" every $625\mu s$

²Because of the frequency hopping scheme, it is probably assumed that these strong interferers do not occur simultaneously for a significant time interval

Function	Parameter	Value
ADC	f_{AD} [Ms/s]	60, 80 or 100
	# Bits	unknown
Analog front-end output	Chunks	10 or 20 MHz
	Rate [Ms/s]	f_{AD}
Filters	Type	FIR/IIR ?
	Phase	Exactly linear ?
	Ripple [dB]	unknown
	Transition bands	Don't care ?

Table 2.1: Parameters common to both Bluetooth and HiperLAN/2 channel selection - part I

to a desired carrier frequency or to baseband. Initial assumptions are that the demodulator will require the channel to be at a certain $f_{demod} > 0$, i.e. a band-pass signal. Now the subtle distinction can be made between the *low IF* and *IF* scenario's discussed in section 2.2. Suppose the demodulator requires the selected channel centered at a carrier frequency $f_{demod} = 1$ MHz. If the signal chunk from the analog front-end has the first channel at frequency $f_{start} > f_{demod}$, the "target" frequency is "clear" (referring to the "empty spot" at $f = 1$ MHz in figure 2.5(c)). In other words, no filtering is required to remove other channels or interferers around f_{demod} ³.

Sample rate conversion

The symbol rate of a single Bluetooth channel is 1 Mbps. With an 80 Ms/s ADC this means 80 samples per symbol. Processing 80 samples to decide on whether a transmitted bit was "0" or "1" is very labor intensive and inefficient. Common demodulators do not require such high rates and 8 (or another low integer number) samples per symbol is a more likely situation. Therefore a rate changer will also be necessary in the digital channel selection system.

2.6 Recapitulation of known parameters

The general requirements of the digital channel selection for both Bluetooth and HiperLAN/2 reception have now been discussed. Based on this information, a functional system architecture can be derived. There are three basic functions to consider: filtering, frequency translation and sample rate conversion (see figure 2.9). The known and unknown parameters common to both channel selection systems are listed in table 2.1. In the conclusions of the next chapter, some of the questions are answered and listed in Part II. The sample rate of the input signal $z[n]$ is equal to f_{AD} . The sample rate of output signal $d[n]$ is f_{AD}/M , where M is the decimation factor of the sample rate converter. The detailed filter specifications for Bluetooth and HiperLAN/2 are discussed in sections 2.4 and 2.4.

HiperLAN/2

HiperLAN/2 channel selection is relatively straightforward for scenario 1. No frequency translation is necessary (in the digital part) and the quadrature inputs both pass through a low-pass filter, decimator and are ready for demodulation. Scenario's

³The carrier frequency f_{demod} is the frequency of the selected channel after mixing. Thus a second IF is used and the receiver is of the *heterodyne* type

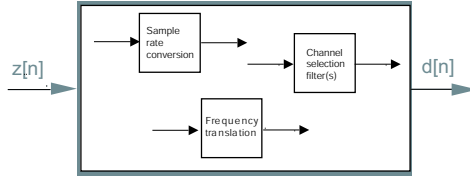


Figure 2.9: Sub-blocks of digital channel selection system

Function	Parameter	Value
Demodulator	Input	Complex
	Rate [Ms/s]	f_{AD}/M ($n \cdot 20Ms/s$?)
	f_{demod} [MHz]	0
Scenario 1		
Analog front-end output	Quadrature	Yes
	Frequency translation	No
Filters	Complex	Maybe
Scenarios 2 and 3		
Input signals	Quadrature	Maybe
	Frequency translation	Yes
Filters	Complex	Maybe

Table 2.2: HiperLAN/2 requirements - Part I

2 and 3 add a frequency translation to the process. Table 2.2 lists the known and unknown parameters so far.

Bluetooth

Detailed filter specifications for the magnitude response of band-pass Bluetooth signals are frequency translated versions of those specified in figure 2.8. Linear phase response is assumed to be of large importance for correct demodulation of the Bluetooth signals. As the carrier frequency of a Bluetooth signal changes regularly, flexible filters must be found and/or additional frequency translation techniques applied. In table 2.3, the currently known and unknown design parameters are listed.

Function	Parameter	Value
Demodulator	Input	Real
	Rate [Ms/s]	f_A/M
	f_{demod} [MHz]	$\leq f_A/M$
Scenario 1		
Analog front-end output	Quadrature	Yes
Filters	Complex	Maybe
Scenarios 2 and 3		
Input signals	Quadrature	Maybe
Filters	Complex	Probably not

Table 2.3: Bluetooth requirements - Part I

3

Channel selection - detailed requirements

3.1 Introduction

This chapter contains more detailed information about the chosen receiver architecture. It is meant as an addition to the previous chapter, and discusses the design choices made in response to the design choices made in the SDR project for the analog front-end and both demodulators. The first section about the analog front-end goes into more detail regarding the incoming signals and the influence on the design choices for the channel selection system. Then, requirements imposed by the demodulator are discussed and the consequences for the channel selection system under design.

3.2 Analog front-end

The currently proposed architecture for the analog front-end is shown in figure 3.1 [6]. It is based on *quadrature down conversion*, meaning that two signal paths will be present at the channel selection input. 20 MHz chunks are down-converted to baseband, which was discussed in the previous chapter as scenario 1 (in section 2.2). The quadrature down conversion method [15], [9], [7], [2] uses the architecture

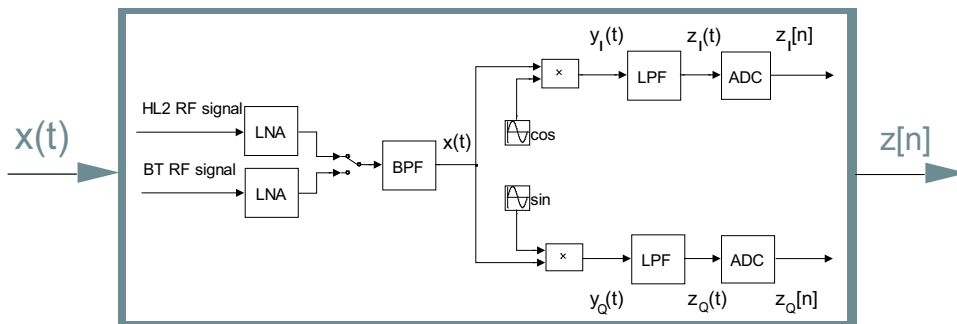


Figure 3.1: Analog front-end demonstrator architecture

shown in figure 3.1. This is the analog front-end block of figure 2.2 in it's expanded form. From now on, $x(t)$ is defined as the real band-pass signal *after* the band-pass filter and LNA. The signal is shifted to baseband using a quadrature down mixer.

The complex injection [13] $\tilde{L}O(t) = e^{j2\pi f_{LO}t}$ is realized by using two signal paths. These are called *In-phase* and *Quadrature* path. The syntax used is defined as:

$$\tilde{L}O(t) \equiv (LO_I(t), LO_Q(t)) \equiv LO_I(t) + j \cdot LO_Q(t) \quad (3.1)$$

The complex injection can be described as:

$$\tilde{L}O(t) = e^{j2\pi f_{LO}t} = \cos(2\pi f_{LO}t) + j \sin(2\pi f_{LO}t) \quad (3.2)$$

Thus, the quadrature mixer uses two local oscillators that are exactly 90° out of phase. This is represented by a sine and a cosine. Verification can be done by adding their (complex) constituents given below using eq. 3.1.

$$LO_I(t) = \cos(2\pi f_{LO}t) = \frac{e^{j2\pi f_{LO}t} + e^{-j2\pi f_{LO}t}}{2} \quad (3.3)$$

$$LO_Q(t) = \sin(2\pi f_{LO}t) = \frac{e^{j2\pi f_{LO}t} - e^{-j2\pi f_{LO}t}}{2j} \quad (3.4)$$

Their amplitude spectra are shown in figure 3.2 (a) and (b). To see how the complex mixer operation results in an uneven output spectrum, eq. 3.2 is shown graphically in figures 3.2 (c) and (d). In (c) the Q path is placed 'in quadrature' by multiplying with j . The resulting uneven spectrum is shown in figure 3.2(d). The magnitude

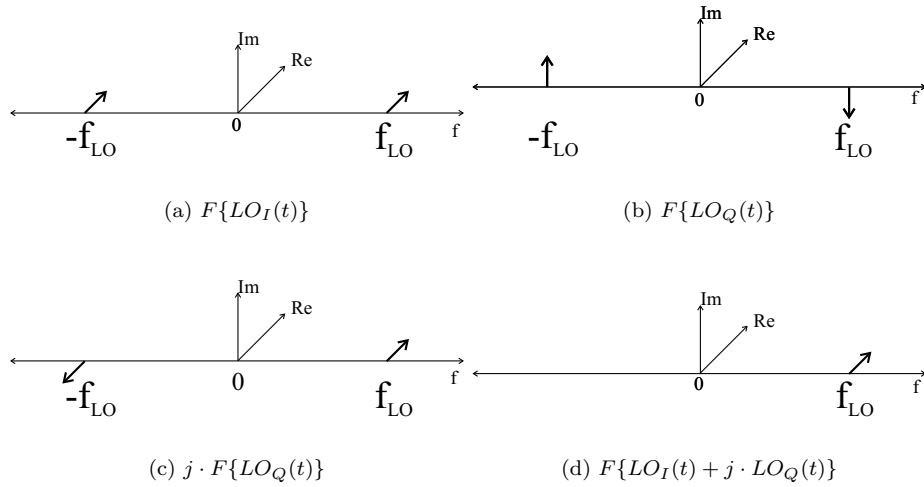


Figure 3.2: Amplitude spectra of the complex mixer constituents

spectra of the RF signal is shown in figure 3.3(a). The magnitude spectra of the local sine and cosine oscillators are identical. Therefore, only $|LO_I(f)|$ needs to be shown in figure 3.3(b). The resulting down mixed signals I and Q also have identical magnitude spectra. $|Y_I(f)|$ is shown in figure 3.3(c). The only difference is that the phase of the I path is 90° behind on Q. With these mathematical principles, the resulting signal obtained by quadrature down conversion of the band-pass signal $x(t)$ is called $\tilde{y}(t)$:

$$\tilde{y}(t) = x(t) \cdot e^{j2\pi f_{LO}t} \quad (3.5)$$

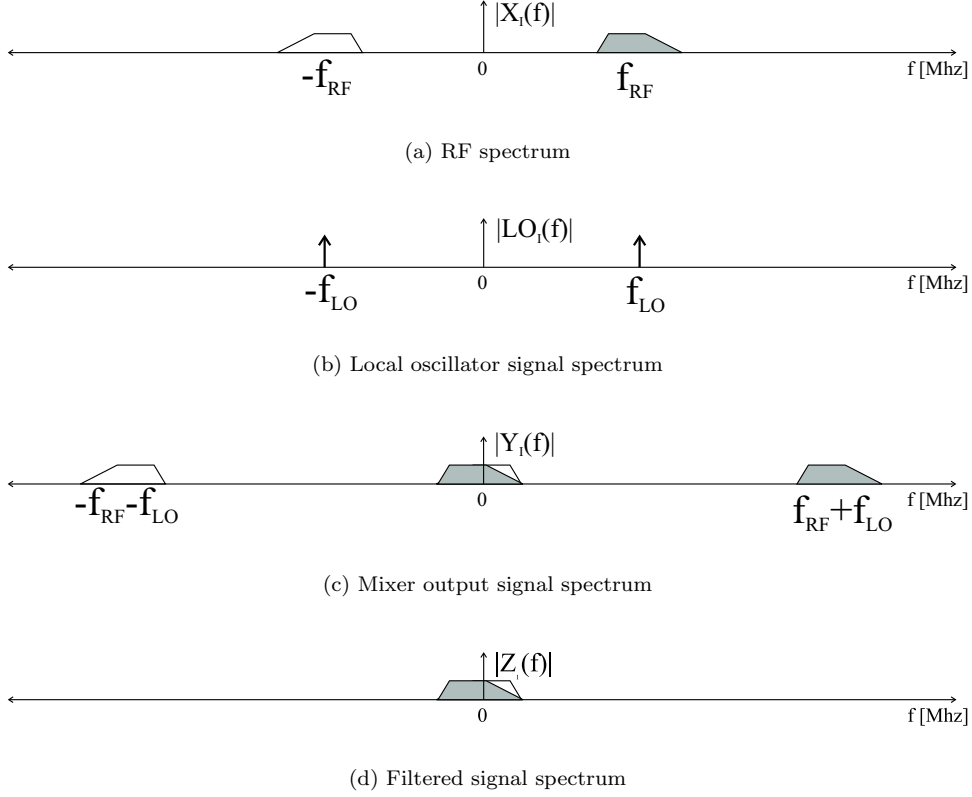


Figure 3.3: Magnitude spectra of analog down mixer signals

It can be readily verified that $\tilde{Y}(f)$ is the frequency shifted (low-pass equivalent) of $X(f)$ by taking it's Fourier transform:

$$\tilde{Y}(f) = F\{x(t) \cdot e^{j2\pi f_{LO}t}\} = X(f - f_{LO}) \quad (3.6)$$

The complex signal $\tilde{y}(t)$ consists of $y_I(t)$ and $y_Q(t)$, defined by the following relations:

$$y_I(t) = x(t) \cdot \cos(2\pi f_{LO}t) \quad (3.7)$$

$$y_Q(t) = x(t) \cdot \sin(2\pi f_{LO}t) \quad (3.8)$$

Fourier analysis of the individual paths reveal the images at $f + f_{LO}$ and $-(f + f_{LO})$:

$$\begin{aligned} F\{y_I(t)\} &= F\{x(t) \cdot \cos(2\pi f_{LO}t)\} \\ &= F\left\{x(t) \cdot \left[\frac{e^{j2\pi f_{LO}t} + e^{-j2\pi f_{LO}t}}{2}\right]\right\} \\ &= \frac{1}{2}[X(f - f_{LO}) + X(f + f_{LO})] \end{aligned} \quad (3.9)$$

N	60	80	100
1	3	4	5
2	$\frac{3}{2}$	2	$\frac{5}{2}$
3	$\frac{3}{4}$	1	$\frac{5}{4}$

Table 3.1: HiperLAN/2 decimation factors

$$\begin{aligned}
F\{y_Q(t)\} &= F\{x(t) \cdot \sin(2\pi f_{LO}t)\} \\
&= F\left\{x(t) \cdot \left[\frac{e^{j2\pi f_{LO}t} - e^{-j2\pi f_{LO}t}}{2j}\right]\right\} \\
&= \frac{1}{2j}[X(f - f_{LO}) - X(f + f_{LO})] \\
&= \frac{1}{2}j[-X(f - f_{LO}) + X(f + f_{LO})]
\end{aligned} \tag{3.10}$$

The unwanted images $f + f_{LO}$ and $-(f + f_{LO})$ are removed by applying low-pass filters (depicted in figures 3.3(c) and (d)). The resulting complex signal is called $\tilde{z}(t)$. After AD conversion, the complex signal $\tilde{z}(t) = (z_I(t), z_Q(t))$ is sampled at instances $t = nT$, where T is the sample time $1/f_{AD}$. The representation in the digital domain is defined as $(z_I[n], z_Q[n])$. Graphical representation of the procedure is shown in figure A.1 on page 64.

3.3 Requirements imposed by the demodulator

HiperLAN/2

The HiperLAN/2 demodulator is more power efficient if its inputs have a sample rate of $N \cdot 20$ MHz [22]. The decimation factor M_{HL} is therefore:

$$M_{HL} = \frac{f_{AD}}{N \cdot 20}$$

where N is an integer. For the f_{AD} 's under research this means that several configurations involve non-integer decimation. This is shown in table 3.1. Non-integer N effectively means interpolation, an operation that increases the data-rate, but does not add information. The following table shows the decimation factors for different scenario's: The channel selection filters should use both I and Q paths. Using two independent or identical real filters or a complex structure as in [17] will be researched.

Bluetooth

For Bluetooth signals, the currently proposed demodulator requires the selected channel in the form of a real band-pass signal. The input sample rate of the demodulator is defined as $f_{demorate}$, and the center frequency of the selected channel f_{demod} . The following must apply [10]:

$$f_{demorate} \geq 8MHz \tag{3.11}$$

and

$$f_{demod} = \frac{f_{demorate}}{4} \tag{3.12}$$

f_{demod} [MHz]	M	f_{AD}		
		60	80	100
2	8	$\frac{15}{2}$	10	$\frac{15}{2}$
2.5	10	6	8	10

Table 3.2: Bluetooth decimation factors

To minimize processing, f_{demod} must be kept as low as possible. $f_{demod} = 2$ MHz with 8 samples per symbol or with $f_{demod} = 2.5$ MHz with 10 samples per symbol will be researched. The decimation factor M (M_{BT} for Bluetooth signals) thus becomes:

$$M_{BT} = \frac{f_{AD}}{f_{demod}} \quad (3.13)$$

With $f_{AD} = 80$ MHz, M_{BT} must be 10 or 8 respectively. For the other f_{AD} 's under research the consequences are shown in table 3.2.

3.4 Channel selection system

The currently proposed analog front-end and demodulator architectures have several implications for the channel selection system. As shown in figure 3.4, two separate demodulators are used, the HiperLAN/2 demodulator requiring quadrature inputs, and the Bluetooth demodulator doesn't. However, the incoming signals are in quadrature, so for Bluetooth a suitable conversion method must be chosen. The following sections will discuss the matters separately for HiperLAN/2 and Bluetooth.

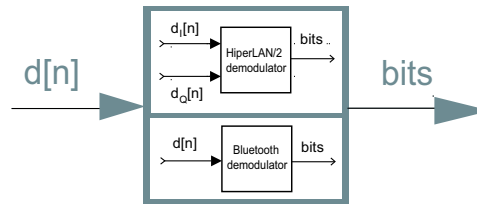


Figure 3.4: Demonstrator demodulators

HiperLAN/2

With the proposed demonstrator architecture, the filter requirements of section 2.4 can be used. Both I and Q paths can be filtered independently or in quadrature with a complex filter structure (shown in figure 3.5). Generally, full complex filters have 2 filters for each signal (one for the real part of the complex filter coefficients and one for the imaginary part) [13]. The advantage of complex filters is that frequency responses with uneven symmetry can be achieved. However, since the HiperLAN/2 channel selection requirements do not specify this requirement, two identical real filters can be used.

Bluetooth

A chunk of Bluetooth signals is presented at baseband by the analog front-end. The positive and negative spectra of the different channels are occupying the same space

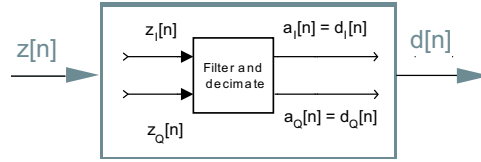
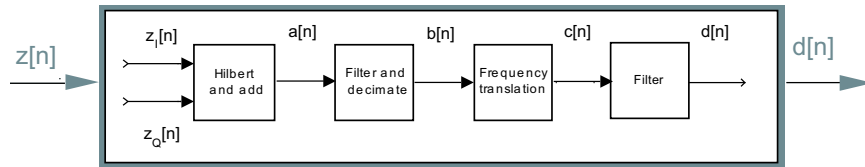


Figure 3.5: HiperLAN/2 channel selection

(as shown in figure 2.5). Both I and Q paths are needed to preserve all information. On the other hand, the demodulator requires a single signal input, containing a real band-pass signal. Thus, somewhere inside the digital channel selection system, I and Q paths must be combined. An important design option is *when* to do this.

As Soon As Possible (ASAP)

With two signal paths at the input, all signal processing operations must be done for both paths. This roughly doubles the amount of work. A first impulse would be to minimize filter operations by combining I and Q paths right away. This can be done by using the Hilbert transform (discussed in Appendix B). By taking the Hilbert transform of one signal path and adding it to the other, the upper or lower sideband is chosen. The sign bit of the adder changes the selection of upper/lower sideband. The consequences of this approach are that frequency translation must

Figure 3.6: Bluetooth **ASAP** channel selection system

be done *after* some filtering, because mixer images of strong interferers can occupy the f_{demod} region. And after mixing the wanted channel to f_{demod} with a real mixer, additional filtering is required to remove the mixer image of the selected channel. This also implies that a channel selection filter (located in the filter and decimate sub-block) must be reconfigured for every channel (and thus every hop). The filter specifications for Bluetooth channels with carrier frequencies ranging from $f_{demod} = 0.5, 1.5, 2.5, \dots, 9.5$ MHz are frequency shifted versions of figure 2.8. For instance, if the selected channel has $f_c = 2.5$ MHz the specifications are:

- Minimum attenuation ≤ -0.838 MHz: 64 dB¹
- Minimum attenuation at ≤ 0.838 MHz: 54 dB
- Stop band: 1.163 – 1.838 MHz, minimum attenuation: 24dB
- Transition band: 1.838 – 2.163 MHz
- Pass-band: 2.163 – 2.838 MHz
- Transition band: 2.838 – 3.163 MHz

¹The required attenuation of the negative frequencies must be provided by the Hilbert transformer.

Function	Parameter	Value
ADC	$f_{AD}[Ms/s]$	80
Analog front-end output	Chunks	20 MHz

Table 3.3: Parameters common to both Bluetooth and HiperLAN/2 channel selection - part II

- Stop band: 3.163 – 3.838 MHz, minimum attenuation: 24
- Minimum attenuation at ≥ 3.838 MHz: 54 dB
- Minimum attenuation at ≥ 4.838 MHz: 64 dB

As Late A Possible (ALAP)

If the complex signal pair $(z_I[n], z_Q[n])$ is preserved, channel selection filtering can be done by using complex filters. One advantage of this approach is that the wanted channel can be frequency shifted to f_{demod} without worrying about images. With an $f_{AD} = 80$ Ms/s, the fundamental interval of the filters (operating at the same rate) is twice the size of the signal band. All signals in the negative side of the frequency spectrum can be shifted to $-f_{demod}$ and everything in the positive side to $+f_{demod}$. The stronger interference signals are also shifted but because of the available spectral space, they will not fold back into the $\pm f_{demod}$ region. A fixed complex filter then filters out the signal at either $\pm f_{demod}$. After combination of both signal paths the signal spectrum is even again and ready for demodulation. The penalty for this functionality is that a complex filter is up to 4 times larger than a real filter. Furthermore, the local oscillator required for frequency translation must be running faster than the sample rate. A more feasible approach is to do filtering and decimation first, followed by a combined Hilbert and frequency translation. The mixer consists of two local oscillators with a 90 degrees phase difference. Then, the output signals can be added or subtracted to select the upper or lower sideband. This system will be referred to as the **ALAP** model and shown in figure 3.7. The

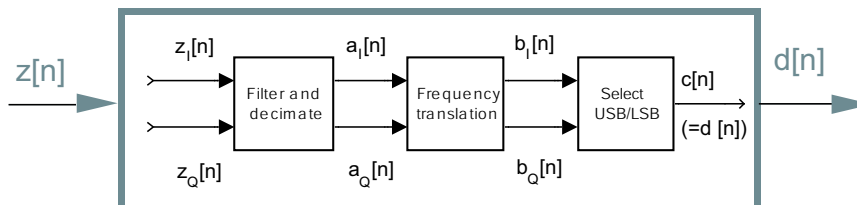


Figure 3.7: Bluetooth **ALAP** channel selection

filter specification are derived the same was as for **ASAP** but now also negative frequencies are used.

3.5 Conclusions

From the information so far, the *common* system specifications in table 3.3 can be derived. The filter type and phase requirements for both Bluetooth and HiperLAN/2 still aren't fixed. FIR (and thus linear phase) filters will be used as a starting point. Referring to table 2.1 (part I) on page 11, two questions have been answered for the common requirements. These are listed in table 3.3 (part II).

Function	Parameter	Value
Demodulator	Input	Complex
	Rate [Ms/s]	20 or 40
	f_{demod} [MHz]	0
Analog front-end output	Quadrature	Yes
	Frequency translation	No
Filters	Complex	No

Table 3.4: HiperLAN/2 requirements - Part II

HiperLAN/2

HiperLAN/2 channel selection remains relatively straightforward. No digital frequency translation is necessary and the quadrature inputs both pass through a low-pass filter, decimator and are ready for demodulation. With $f_{demodrate,HL} = N \cdot 20$ Msps, the decimation factor $M_{HL} = 2$ or 4 . Table 3.4 lists the known and unknown parameters so far. The proposed system for design was discussed in section 3.4, and shown in figure 3.5. The proposed channel selection filters are real. Chapter 4 will discuss the possible contents of the sub-block *filter and decimate*.

Bluetooth

Filter specifications are (a frequency translated version of those) specified in figure 2.8. Phase linearity is still assumed to be of large importance for correct demodulation of Bluetooth signals. Based on filter operations the first goal will be to design a channel selection system with real signals. The complex implementation will be the alternative approach when the real system does not meet requirements. In table 3.5, the known and unknown design parameters are listed. The proposed system for

Function	Parameter	Value
Input signals	Quadrature	Yes
Filters	Complex	Maybe
Decimation	M	10 or 8
Demodulator	Input	Real
	Rate [Ms/s]	8 or 10
	f_{demod} [MHz]	2.0 or 2.5

Table 3.5: Bluetooth requirements - Part II

design is the **ASAP** approach from section 3.4, and shown in figure 3.6. Chapter 4 will discuss the possible contents of the sub-blocks *filter and decimate* and *filter*. In chapter 5 the *frequency translation* sub-block will be addressed.

4

Filter and Decimate

4.1 Introduction

The top level design considerations discussed in chapter 3 have lead to two proposed systems. Both systems contain a *filter and decimate* block of which the implementation will be researched in this chapter. For HiperLAN/2 the proposed system for design was discussed in section 3.4, and shown in figure 3.5. A pair of real low-pass filters will be researched. For Bluetooth the proposed system design is the **ASAP** approach from section 3.4, and shown in figure 3.6. In this case the aim is finding a suitable combination of (real) filters to do channel selection. Note that this chapter contains valuable information for the design of the post-frequency-translation filter, but this filter will not be explicitly discussed until chapter 6. Filter design parameters are discussed, followed by a derivation of a performance figure to compare their merits. Then, several filter types and design methods are discussed. The primary focus will be on **F**inite **I**mpulse **R**esponse (FIR) [8], [21], [12] filters because of their stability¹ and linear phase characteristics. In digital signal processing **C**ascaded **I**ntegrator **C**omb (CIC) filters are also commonly used for decimation purposes and they will also be addressed. Then, a brief investigation into **I**nfinite **I**mpulse **R**esponse (IIR) filters is done.

4.1.1 Design parameters

To design a filter, the specifications must be translated into parameters for the design. The following terminology is used (as in [21]). Strictly speaking, the term *frequency* and the unit *Hertz* may only be used in the analog domain. But, for easier comprehension and more intuitive filter design, these terms will also be associated with the digital domain. Filter operations are now done on arrays of numbers, which are sampled (and quantified) representatives of the original analog signal. The sample time is the inverse of the sample-rate (or -frequency) of the AD converter. The operating frequency of the digital filter defines its fundamental (*Nyquist*) interval. Digital filters are specified and designed relative to their operating rate. If the digital filter operates at the sample frequency $f_{filter} = f_{sample}$, it's fundamental interval ranges from $-f_{filter}/2$ to $f_{filter}/2$. This can be related to the *angular* frequency interval $-\pi$ to π (*rad/s*). The pass- and stop-band *frequencies* are thus normalized and do not specify numbers in the (analog) unit Hz². Other design parameters (that are also illustrated in figure 4.1) are defined as follows:

¹FIR filters do not have feedback and therefore do not oscillate, even with truncated coefficients

²Although it is sometimes more intuitive to talk about digital filters as if they were specified in the analog domain. In this report too, familiar terms like Hertz will sometimes be used.

Peak pass-band ripple: δ_p :

$$\delta_p = 10^{\frac{A_p}{20}} - 1 \quad (4.1)$$

in [dB]:

$$A_p = -20 \log_{10}(1 - \delta_p) \quad (4.2)$$

Minimum stop-band attenuation A_s (in [dB]):

$$A_s = -20 \log_{10} \delta_s \quad (4.3)$$

Peak stop-band ripple δ_s :

$$\delta_s = 10^{-\frac{A_s}{20}} \quad (4.4)$$

Normalized frequency definition of digital filters:

$$\Omega = \omega \cdot T_{sample} = 2\pi f \cdot T_{sample} = 2\pi \frac{f}{f_{sample}} \quad (4.5)$$

Transition bandwidth ($\Delta\Omega$) relative to the fundamental interval π (in radians):

$$\Delta\Omega = \Omega_s - \Omega_p \quad (4.6)$$

Here, $0 \leq \Omega \leq \pi$. This is analog to a specification in f_p and f_s , where $0 \leq f_{p,s} \leq f_{sample}/2$. For digital filters in this chapter f_{filter} will be used in stead of f_{sample} or f_{AD} , because the filters are not always operating at the sample frequency. The normalized dimensionless transition bandwidth δf ($\delta f \in [0, 1]$) is defined as:

$$\Delta f = \frac{f_s - f_p}{f_{filter}} (= \Delta\Omega) \quad (4.7)$$

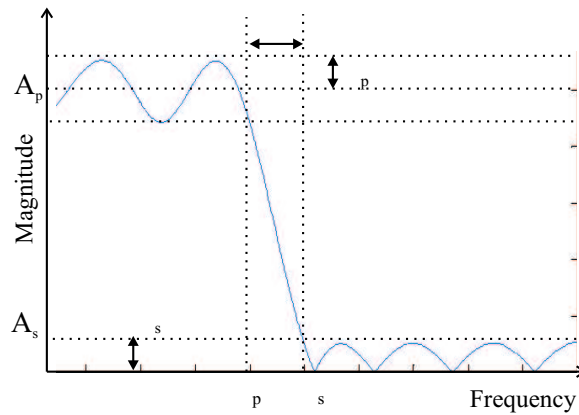


Figure 4.1: (Real) FIR filter design parameters

4.1.2 Filter performance

To compare different filter designs and structures, a **Performance Figure** is needed. In this section a PF will be derived to compare design. An important parameter is the amount of (nonzero) filter coefficients that must be multiplied with the incoming

samples. For FIR filters, this amount is equal to the impulse response length. The amount of multiplications and additions performed per input sample is another parameter. Symmetrical FIR filters for instance can (in some cases) be implemented with half the amount of multiplications per second. Other filters are optimized so they do not need multiplications at all. The following subsections will define how these properties are used.

Filter coefficients

The filter coefficients are generally stored in registers with delay lines in between. A FIR filter of *order* N has $N+1$ filter coefficients in the feed forward path. A *direct form* FIR filter structure visualizes this best (see figure 4.2(a). This is a 2^{nd} order filter (two delay elements) with 3 coefficients. An IIR filter of order N can have up to $N+1$ coefficients in the feed forward *and* feed-back path (see figure 4.2(b)). This can amount up to $2 \cdot (N + 1)$ filter coefficients. To reduce the amount of adders the IIR filter structure can also be implemented in *canonical form* (as shown in figure 4.2(c)).

Operations per second

The calculation of one output sample involves multiplying $(N+1)$ previous samples with the filter coefficients and adding their results. Thus, for each input sample, $N+1$ multiplies and $N+1$ accumulates are done. If symmetric filter coefficients are used, in common architectures one Multiply **AC**cumulate operation can process 2 input samples [19]. So for each input sample $(N + 1)/2$ MACs are done. Other filter implementations are optimized to remove multiplications, leaving only additions and/or subtractions. Therefore, this thesis will talk about ACs/s (Accumulates per second), and MULTs/s (MULTiplications per second) and MACs. The computational complexity of a filter can thus be defined as a weighed³ sum of MACs/s, ACs/s and MULTs/s. The operating rate of the filter is equal to the incoming number of samples (per second). It is defined by the operating frequency⁴ of the filter f_{filter} . Example: a FIR filter of order 32 processes 8 million samples per second using only MAC operations will have a performance figure of:

$$PF = (N + 1) \cdot f_{filter} = 33 \cdot 8 \cdot 10^6 = 264 \cdot 10^6 \text{ MACs/s} \quad (4.8)$$

If the filter implementation takes advantage of the symmetric property this is divided by two:

$$PF = \frac{(N + 1) \cdot f_{filter}}{2} = 132 \cdot 10^6 \text{ MACs/s} \quad (4.9)$$

Now if the filter is followed by decimation, polyphase implementation can reduce this figure with a factor M (the decimation factor). Choosing $M = 4$ the performance figure thus becomes:

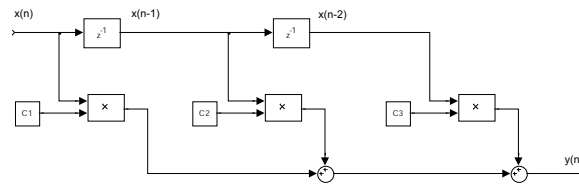
$$PF = \frac{(N + 1) \cdot f_{filter}}{2 \cdot M} = 33 \cdot 10^6 \text{ MACs/s} \quad (4.10)$$

Power consumption

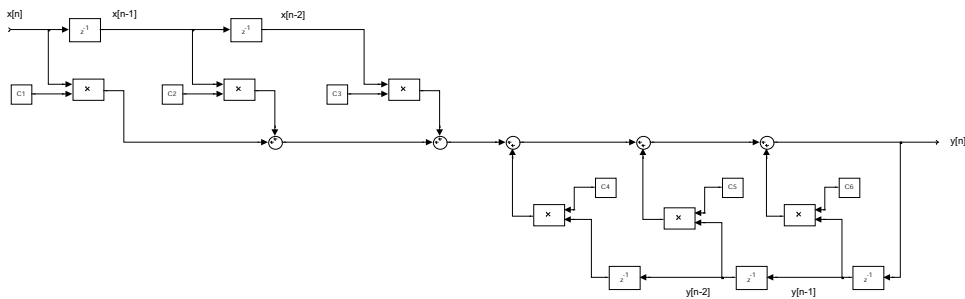
An important design constraint is the power consumption. In this report, it is assumed that the power is directly proportional to the aforementioned PF. In case of

³The weight factors for the performance figures are yet to be determined based on the soft- or hardware that will be used to implement the filters on (FPGA/DSP/GPP)

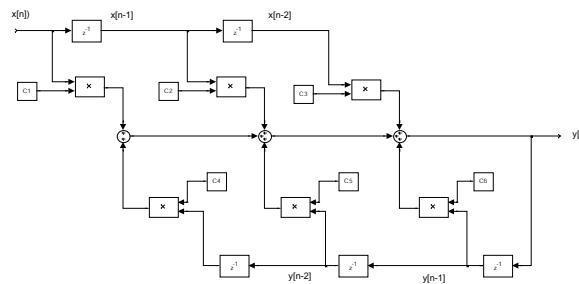
⁴The operating frequency of a filter is equal to the highest sample rate it processes, either at the input or the output.



(a) FIR filter: only feed forward (nonrecursive)



(b) IIR filter: additional feed back (recursive)



(c) IIR filter: reduced # adders

Figure 4.2: 2nd order FIR and IIR filter implementations

hardware implementation, the word lengths are also in important factor. The word length of the input samples will be specified as soon as an AD converter is chosen, which remains to be done in the future. However, as the stated power relation increases or decreases linearly with different word lengths this does not hinder the goal of finding optimal filter systems. Data-sheets of DSP processors usually specify power consumption in terms of several milliwatts per million instruction per second ($mW/MIPS$) at a certain supply voltage. This can also be related to the performance figure of section 4.1.2. FPGA power consumption depends on the amount of configurable logic blocks that are used for a specific design. With a given power figure for a fully "loaded" FPGA board initial estimates can be given.

4.2 FIR

4.2.1 Least squared error

This method optimizes a filter according to an error criterion based on the square of the deviation of the actual response, compared to the desired (ideal) response. The error can be seen as the sum of neglected coefficients, because only a finite number of filter elements is used. Thus, smaller errors are obtained by increasing the filter length. When a direct approximation of an ideal low-pass filter is done using the inverse Fourier transform, the sharp transition bands obtained from long filters suffer from Gibbs' phenomenon [8]. This phenomenon is the overshoot in the amplitude frequency response due to the discontinuity at cut-off and does not reduce to 0 as $N \rightarrow \infty$. By relaxing the constraints on the transition band (smoothing the discontinuity), overshooting is greatly reduced. This is discussed in section 4.2.2. Filter lengths are largely dependent on Δf as defined in eq. 4.7. Reducing the processing speed (f_{filter}) of the digital filter effectively lowers the value for Δf , thus reducing the filter length. Applications of this technique will be further discussed in section 4.2.5.

4.2.2 Windowing

To reduce the effects of truncation of the impulse response, filter coefficients can be *windowed* [21]. The discontinuity of the impulse response is reduced by multiplying the coefficients with a window function. This way the coefficient values gradually decrease to zero. The length of the window equals the number of filter taps. Table 4.1 lists several window types and characteristics [4]. The parameter δ_m is defined as $\min(\delta_p, \delta_s)$. In other words: a large stop-band attenuation automatically requires a small pass-band ripple and vice versa. The shape of the window defines the maximum stop-band attenuation (and thus δ_p). The transition bandwidth of the window filters is defined by the filter order. The Kaiser window is actually a family of windows generated from a common equation (Bessel functions). Given a stop-band attenuation, the β factor is calculated with eq. 4.11. Then, either N is determined from the transition width or vice versa.

Window	δ_p	A_s [dB]	Δf
Rectangular	0.7416	21	0.9/N
Kaiser ($\beta = 2.12$)	0.270	30	1.5/N
Hann (Raised cosine)	0.0546	44	3.1/N
Kaiser ($\beta = 4.55$)	0.0274	50	2.9/N
Hamming	0.0194	53	3.3/N
Kaiser ($\beta = 6.76$)	0.00275	70	4.3/N
Blackman	0.0017	74	5.5/N
Kaiser ($\beta = 8.96$)	0.000275	90	5.7/N

Table 4.1: Windowed filter design characteristics

$$\beta = \begin{cases} 0.1102(A_s - 8.7) & \text{if } A_s > 50 \\ 0.5842(A_s - 21)^{0.4} + 0.07886(A_s - 21) & \text{if } 21 < A_s < 50 \\ 0 & \text{if } A_s < 21 \end{cases} \quad (4.11)$$

4.2.3 Uniform approximation

This design method, also referred to as *equiripple* method [21] aims to minimize the maximal deviation from the desired amplitude frequency response for a given filter

length. A tolerance band may be defined in the pass- and stop-band wherein the approximate amplitude of the frequency response follows a wave-like curve. The minima and maxima of the curve touch the upper and lower limits of the band. The Parks-McClellan ⁵ algorithm finds optimum equiripple linear-phase FIR filters. They are "optimal" in the *minimax* sense of magnitude frequency response. In other words: the allowed error within the pass- and stop-bands is spread across the frequency response. This spreading can be adjusted by changing the weight factors and in the transition band there is no constraint. The algorithm finds the minimum amount of filter coefficients for which the maximum error is within the specified bounds. The maximum error is determined from the error function $E(\Omega)$, defined as:

$$E(\Omega) = H(\Omega) - H_{desired}(\Omega) \quad (4.12)$$

$H_{desired}(\Omega)$ is the magnitude response of the desired filter. By minimizing $|E(\Omega)|$ an optimal (equiripple) filter design is obtained that approximates the desired response within the specified error margin. Estimates of the required filter order based on this method have been formulated by Kaiser (eq. 4.13) and Bellanger (eq. 4.14) [21],[12]. They found:

$$N_{kai} = \frac{-20 \cdot \log_{10} (\sqrt{\delta_p \delta_s} - 13)}{14.6 \Delta f} \quad (4.13)$$

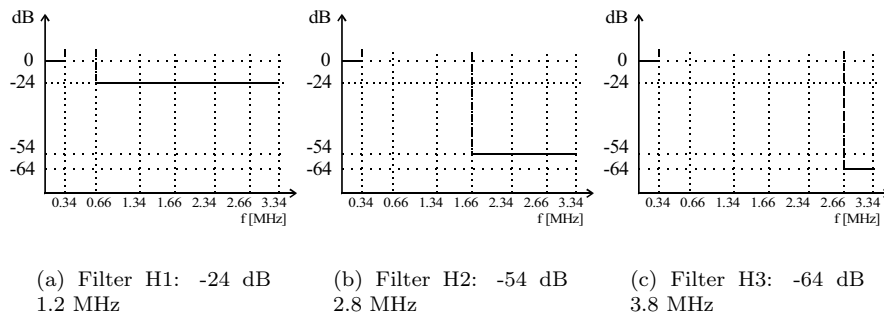
$$N_{bel} = \frac{2}{3} \cdot \log_{10} \left(\frac{1}{10 \delta_p \delta_s} \right) \cdot \frac{1}{\Delta f} \quad (4.14)$$

In these formulae, the estimated filter order N is proportional to the maximum allowable pass-band ripple (A_p/δ_p), stop-band attenuation (A_s/δ_p) and inversely proportional to the transition bandwidth. Strictly speaking, these estimation formulae are only valid for uniform approximation (optimum equiripple) FIR filter designs. However, for each set of parameters (f_p , f_{stop} , δ_p and δ_s) it turns out that an equiripple filter has the smallest possible order N [21]. Hence, these estimations for the filter order can be used as a guideline (minimum boundary) for other FIR filter designs. The filter specifications for Bluetooth and HiperLAN/2 (referring to section 2.4) do not specify the allowed pass-band ripple. Assuming $\delta_p = 0.01$ allows some estimates for N , but the required filter order does have a substantial dependency on the allowed pass-band ripple. Therefore, estimates can change significantly if other values for δ_p were to be used (see figure 4.4). The filter lengths required for the Bluetooth case are unpractical. This is of course due to the small (normalized) transition bandwidth (Δf). To reduce the filter lengths, Δf can be increased by using multi stage and/or multi rate techniques.

4.2.4 Influence of Δf and δ_p on N

The minimum stop-band attenuation (and thus the allowable stop-band ripple) is fixed by the specifications. The two remaining most important parameters determining the estimated required filter order N are the pass-band ripple δ_p and transition bandwidth. The reduction of the filter order as a function of the pass-band ripple and transition band width will now be calculated by using three example filters. These filters are designed using specifications that are loosely based on the Bluetooth low-pass filter requirements of section 2.4. These specifications are shown in figure 4.3 and are only chosen as examples to demonstrate the behavior of the estimation formula for variations in δ_p and ΔF . The stop-band ripple is defined by the stop-band attenuation using the relation from eq. 4.4.

⁵The Parks-McClellan algorithm is also known as the Remez exchange algorithm

Figure 4.3: Filter specifications used for $\delta_p, \Delta f$ influence example

Variations in Δf

Variations of Δf cannot be directly applied because that would change the given filter specifications. Although this is possible in an example such as this, the idea is to use the gained knowledge in the actual design. Therefore the operating frequency of the filter is a variable, and equivalent by the following relation (eq. 4.7):

$$\frac{f_s - f_p}{f_{filter}}$$

In this case, the filter frequency is directly related to the AD converter frequency ($f_{filter} = f_{AD}$). Appropriate values for this project are in the range of 60 to 100 MHz. The fundamental interval of the filters ($f = 0..f_{filter}/2$) thus ranges from 30 to 50 MHz. By increasing f_{filter} , the normalized transition bandwidth Δf decreases and the estimated required filter order goes up. The values for the estimated filter order N are calculated using Bellangers formula (refer to eq. 4.14)). The results are shown in figure 4.4(a). Three lines are plotted for the three different filters as a function of the filter frequency. The transition bandwidth of H1 is very small compared to the fundamental interval of the filter and this causes the required filter order to be high. For H2 and H3, Δf is larger, resulting in lower filter orders. Note that this is despite the larger required stop-band attenuation. The gradient indicates the sensitivity of the order to a change in the transition band-width. In estimated filter order is larger for the sharpest filter (H1) and thus benefits most from a relative decrease of Δf .

Variations in δ_p

Figure 4.4(b) shows the influence of the allowed pass-band ripple at a fixed sample rate of 60 MHz for the same three filters. Again, H1 benefits most from variations in the parameter. Its estimated order reduces by 50% with a factor 10 increase of δ_p . For H2 and H3 the allowed stop-band ripple δ_s is smaller and the $\delta_p \cdot \delta_s$ product remains small, allowing less drastic improvements. Thus the conclusion can be drawn that for filters with large stop-band attenuation (resulting in a small δ_s) the magnitude of pass-band ripple is not a significant factor in the given range.

4.2.5 Multi-rate

It has been shown in section 4.2.4 that for the Bluetooth channel selection filters significant size reduction can be achieved by lowering f_{filter} . In digital signal pro-

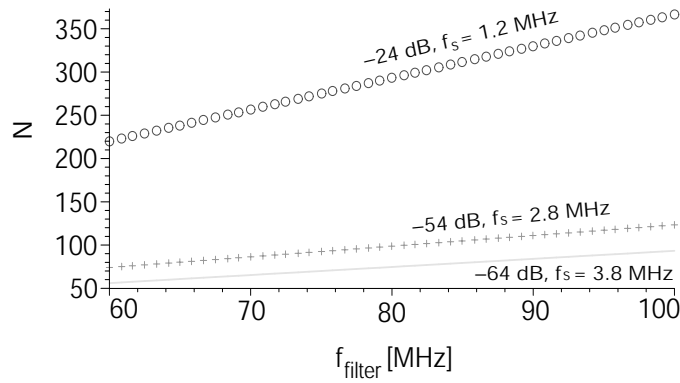
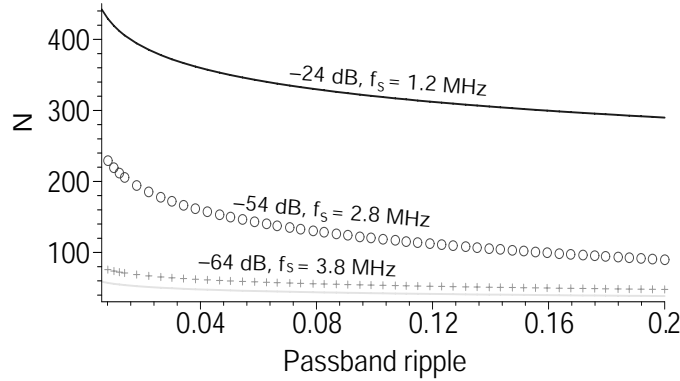
(a) Δf influence, $\delta_p = 0.01$ (b) δ_p influence ($f_{filter} = 60$ MHz)

Figure 4.4: Parameter sensitivities

cessing this can be done by decimation.

Decimation

The device lowering the rate at which input samples arrive is called a decimator [21]. A decimator periodically passes one sample through and discards the rest. For example, a decimation factor $M = 10$ means 1 sample is passed through and 9 are discarded. The operating rate of the decimator output is thus one tenth of its input (eq. 4.15).

$$f_{out} = \frac{f_{in}}{M} \quad (4.15)$$

The consequences of this rate change are alias spectra at multiples of f_{in}/M . Assume a filter system as shown in figure 4.5(d). To demonstrate the behavior of decimation, both filters are initially all-pass (all signals are passed through unchanged). The first filter operates at frequency $f_{filter} = f_{in} = F_{AD}$. At its input, a channel is present near baseband (shown in figure 4.5(a)). It is a real bandpass signal with carrier frequency f_c and having an even spectrum, both positive (grey, $+f_c$) and negative frequency components (white, $-f_c$) are shown. The fundamental

interval of this H_{pre} filter is $-f_{in}/2, f_{in}/2$. At the output of the filter, the signal is decimated by a factor $M = 2$. By reducing the sample rate, aliasing occurs at multiples of the output frequency. This is illustrated in figure 4.5(b), where images of the spectrum are shown at $f_{out} + f_c$ and $-f_{out} - f_c$. Now suppose there is an interferer present at the input with a carrier frequency $f_i > f_{out}$. This is shown in 4.5(c). After decimation, an alias will fold into the region $f_c - f_{out}$. In figure 4.5(d) it is shown that the interferer is now partly indistinguishable from the original signal. To avoid this, the pre-decimation filter (H_{pre}) must have a cutoff frequency $< f_{out}$. H_{pre} is called an anti-alias filter (see also figure 4.5(e)). The advantage of the decimation is that the H_{post} filter operates at a M times lower rate, thus increasing Δf M times. Significant reductions on filter order can thus be achieved by multi-rate filtering. Qualitative and quantitative analysis of this property for both Bluetooth and HiperLAN/2 systems will be discussed in the following sections. Note that the purpose of decimation (lowering the operating frequency of the filter) seems to apply only to the H_{post} filter. This is not entirely true and will be discussed in section 4.2.6.

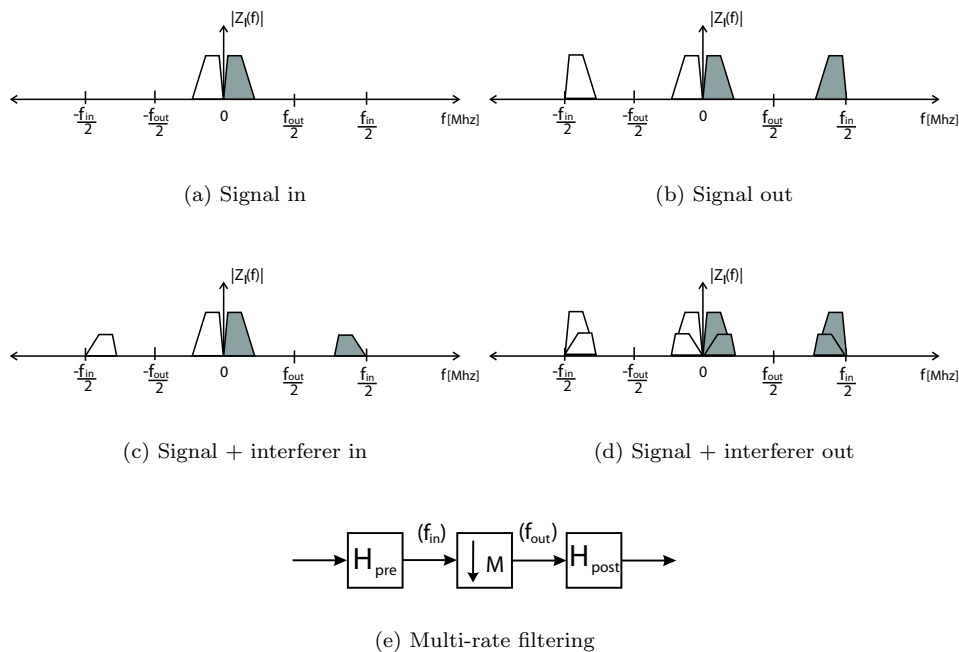


Figure 4.5: Decimation and possible aliasing ($M = 2$)

Qualitative analysis

It is clear that the amount of filter operations performed by the post-decimation filter will steadily decrease as the decimation factor M increases. The opposite is true for the pre-filter. The total total filter operations performed (the sum of both) has a minimum at a certain decimation factor. Note that the pass-band ripple δ_p of the resulting filter can be twice that of the individual filters (see definition in figure 4.1 and [21]). Therefore, the requirement for each stage is δ_p/N , where N is the number of cascaded filters (in this case $N = 2$). The optimal decimation factor can be found with some algebraic manipulations. Recall the formula for FIR filter

order N (eq. 4.14):

$$N \approx \frac{2}{3} \cdot \log_{10} \left(\frac{2}{10\delta_p\delta_s} \right) \cdot \left(\frac{1}{\Delta f} \right)$$

For a given filter specification, this can be reduced to:

$$N \approx \frac{\chi}{\Delta f} \text{ where } \chi > 0$$

Now recall the definition of the transition bandwidth Δf (eq. 4.7):

$$\Delta f = \frac{f_{stop} - f_{pass}}{f_{filter}}$$

The post decimation filter operates at a frequency $f_{filter,post} = f_{out} = f_{in}/M$. Substituting into the approximation formula:

$$N_{post} \approx \frac{\chi \cdot f_{in}}{(f_{stop} - f_{pass}) \cdot M}$$

Thus, for a given filter specification and input frequency, the order of the post decimation filter is inversely proportional to M :

$$N_{post} \propto \frac{1}{M}$$

The amount of filter operations performed by this filter, defined as the filter order multiplied by the operating frequency (in short: *FOPS*), is given by:

$$FOPS_{post} \approx N_{post} \cdot \frac{f_{in}}{M} \approx \frac{\chi \cdot f_{in}^2}{(f_{stop} - f_{pass}) \cdot M^2} \propto \frac{1}{M^2}$$

The *FOPS* of the post-decimation filter thus decrease quadratically with M . The cutoff frequency of the pre-filter must (at the least) be equal to the output frequency after decimation. The pass-band of the pre-filter is taken equal to the that of the post-filter. The stop-band of the pre-filter is chosen to exactly cancel (attenuate) the alias of the post-filter (see figure 4.6). The Δf_{pre} can thus be defined as:

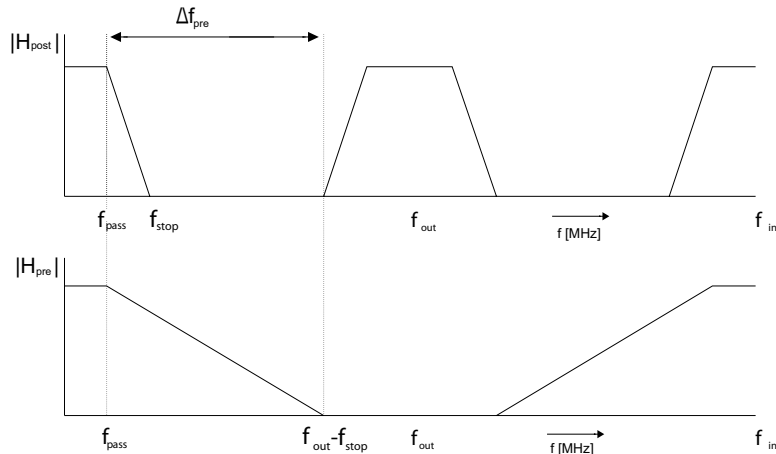


Figure 4.6: Anti aliasing filter specifications

$$\Delta f_{pre} = \frac{f_{out} - f_{stop} - f_{pass}}{f_{in}}$$

Substitute in the estimation formula and assuming $f_{stop} + f_{pass} \ll f_{in}$:

$$N_{pre} \approx \frac{\chi \cdot M}{1 - M \cdot \left(\frac{f_{stop} + f_{pass}}{f_{out}} \right)} \propto M$$

Operating at the (constant) input rate f_{in} , the expression for the $FOPS_{pre}$ becomes:

$$FOPS_{pre} \approx N_{pre} \cdot f_{in} \approx \frac{\chi \cdot M \cdot f_{in}}{1 - M \cdot \left(\frac{f_{stop} + f_{pass}}{f_{in}} \right)} \propto M$$

So while the pre-filter operations *increase linearly* with M, the post-decimation filter operations *decrease quadratically* ! Thus, for given filter specifications an optimal decimation factor M can be found for which $FOPS_{pre} + FOPS_{post}$ is minimal. $FOPS_{total}$ is a parabolic function (valley):

$$FOPS_{total} \approx \frac{\chi'}{M^2} + \chi'' \cdot M \text{ where } \chi', \chi'' > 0$$

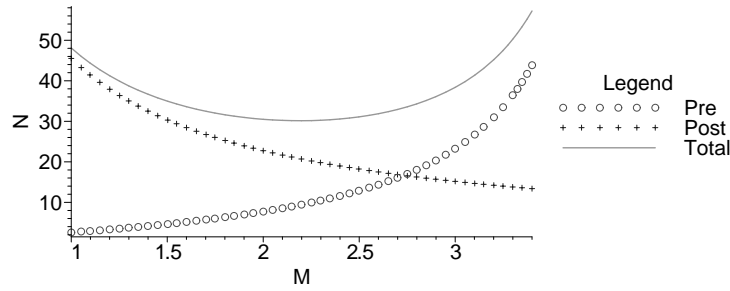
The minimum is found by taking its derivative and finding the roots.

HiperLAN/2 decimation

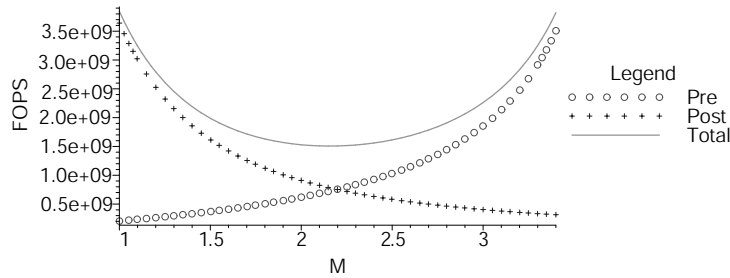
With the known parameters for HiperLAN/2, the optimal decimation factor M for a 2 filter system can be calculated with the aforementioned formulas. Referring to section 2.4 the parameters are: $f_{pass} = 8.3$, $f_{stop} = 11.7$ MHz, $\delta_p = 0.01$ and $A_s = 32$ dB ($\delta_s = 2.5 \cdot 10^{-2}$). The stop-band attenuation is chosen to be 32 dB because the pre- and post-filter responses will add up to the required 51 dB attenuation as total filter response. The results in figures 4.7(a) and (b) show that for HiperLAN/2 a decimation factor of $M = 2$ is optimal for both combined filter order and performance. The decimation factors permitted by the requirements of table 3.4 on page 20 are 2 and 4, so based on the current calculations $M = 2$ is chosen. The proposed filter system for HiperLAN/2 will thus be that of figure 4.7(c). The first low-pass filter (LPF1) is an anti-alias filter and the second low-pass filter (LPF2) performs the sharp channel selection filtering.

Bluetooth decimation

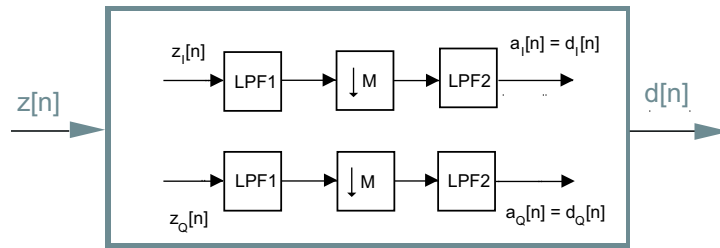
The wanted channel has a carrier frequency $f_c = 0.5$ MHz. The input rate is the sample rate of the AD converter $f_{in} = f_{AD} = 80$ MHz. A channel selection filter is designed with $f_{pass} = 0.8$, $f_{stop} = 1.2$ MHz, $\delta_p = 0.01$ and $A_s = 64$ dB ($\delta_s = 6.3 \cdot 10^{-4}$). The stop-band attenuation is chosen to be 64 dB, which may seem a bit excessive. The two resulting filters will both attenuate the signal 64 dB in the stop-band, and intuitively a requirement of $\approx 64/2 = 32$ dB is enough. However, recalling the filter specifications (of section 2.4 on page 9): a 40 dB stronger interferer may be present only 3 MHz away at carrier frequency $f_i = 3.5$ MHz. A minimum order (equiripple) low-pass filter with a transition band from 0.8 to ≈ 8.8 MHz and a required stop-band attenuation of 64 dB attenuates the signal with carrier frequency f_i with only 5 dB. Specifying a stop-band attenuation of -32 dB reduces this to ≈ 2.8 dB. Thus, the transition band of the pre-filter does not guarantee sufficient attenuation of strong interferers and the post filter should have a stop-band attenuation of at least 60 dB. [10pt] In figures 4.8(a) and (b) the resulting estimated filter order and FOPS are shown for these parameters. The



(a) Filter order vs M



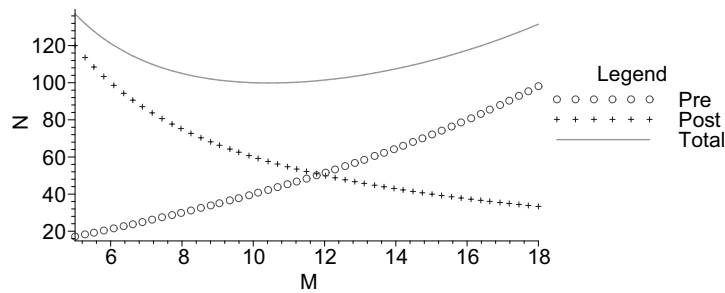
(b) Filter operations vs M



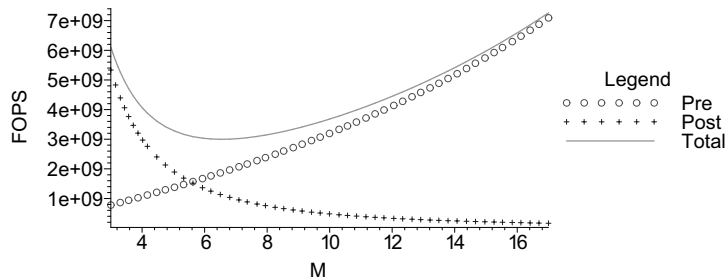
(c) Proposed HiperLAN/2 filter structure

Figure 4.7: HiperLAN/2 multi-rate

minimum total filter order is obtained around $M = 10$ and minimal FOPS around $M = 6$. The decimation factor M is constrained by the requirements of table 3.5 on page 20. From these available options and based on the current considerations, $M = 8$ yields the optimal 2 filter channel selection system with respect to total filter operations. However, as the Bluetooth channel is not always at $f_c = 0.5$ MHz, the design of an optimal filter system is not as straight forward as for HiperLAN/2. In the event that the wanted channel has a carrier frequency $f_c = 9.5$ MHz, the pass-band of the pre filter must be ≈ 10 MHz wide. In this case, the anti-alias requirement of figure 4.6 is breached or the transition band of the pre filter must be very small. In addition, the Nyquist interval of the post filter after a decimation by 8 ranges from -5 to 5 MHz. If the pre filter is simply a low-pass filter with cut-off around $f_{cutoff} = 10$ MHz, this causes tremendous aliasing. Thus, for Bluetooth channel selection either the decimation ratio must be factored or the pre filter must



(a) Filter order vs M



(b) Filter operations vs M

Figure 4.8: Bluetooth multi-rate filtering

be band-pass. The following section discussing polyphase implementation of filters will lean the scale towards factoring of M . The pre-filter will then take the role of anti-alias filter for the first decimation.

4.2.6 Polyphase filters

If a filter is directly followed by a decimator, a lot of the calculated filter output values are discarded. To avoid these unnecessary calculations, filter designs can be modified using the Noble identities [12],[21]. These are shown in section C for quick reference. The pre filter in the configurations of figure 4.5(a) can be implemented using a *transversal* structure [12],[21],[19]. Using the aforementioned identities an efficient structure is obtained, shown in 4.9. Also based on this identity and having the same amount of filter operations is the polyphase structure (see figure 4.10). By performing the decimation before filtering, the required amount of calculations is reduced by a factor M . Thus, combining a filter with a subsequent decimation reduces the filter operations significantly.

HiperLAN/2 filter and decimate (FIR-only)

This method can be used to reduce the filter operations performed by the HiperLAN/2 anti-alias filters of figure 4.7(c). The required filter operations based on theoretical (filter) specifications (as described in section 2.4) are as listed in table 4.2. The pass- and stop-bands are calculated using the specifications of figure 4.6.

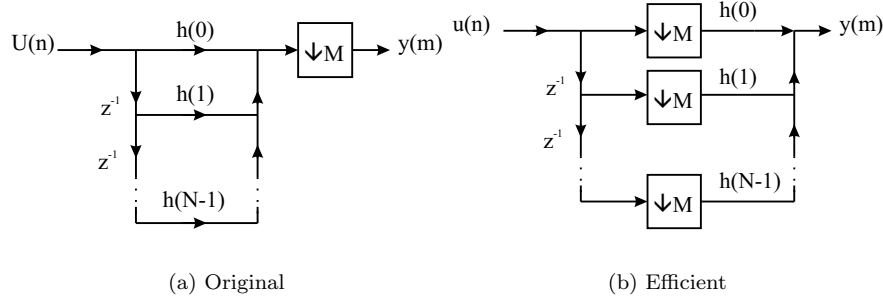


Figure 4.9: Transversal filter structure

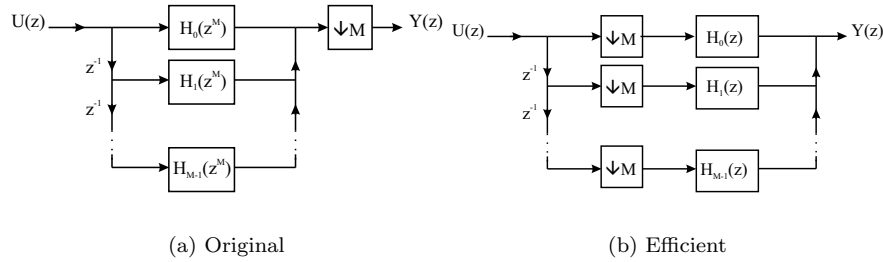


Figure 4.10: Polyphase filter structure

The FIR order is given for an individual LPF1 or LPF2 but the PF⁶ listed is the sum of both filters. The total PF of the HiperLAN/2 filter and decimate system is the sum of the PFs of the individual filters: $360 + 960 = 1320$ MMAC/s. Their magnitude responses are shown in figure 4.11.

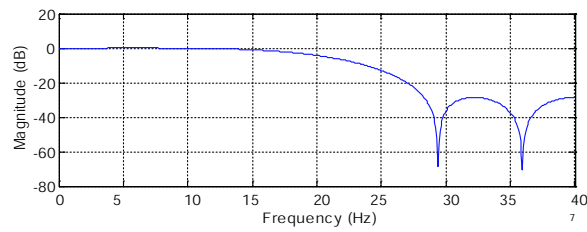
Bluetooth filter and decimate (FIR-only)

For the pending Bluetooth multi-rate problem this approach leads to the following considerations: the decimation factor $M = 8$ can be divided into $M1 \cdot M2 = 8$ or even $M1 \cdot M2 \cdot M3 = 8$. Two stage decimation with $M1 = 4$ and $M2 = 2$ reduces the signal bandwidth from 80 to 20 MHz after the first stage. The pre filter is then a low-pass filter with cut-off near 10 MHz. The post filter will then be a band-pass filter with Nyquist interval ranging from -10 to 10 MHz. This also rules out the decimation factor $M = 10$, where the Nyquist interval would be from

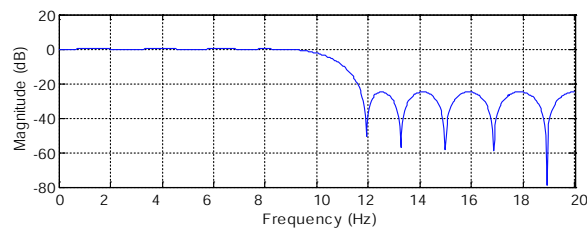
⁶For the derivation of the performance figure please refer to section 4.1.2.

Parameter	LPF1 (2x)	LPF2 (2x)
$\Omega_p (f/f_{filter})$	0.10 (8.28/80)	0.21 (8.28/40)
$\Omega_s (f/f_{filter})$	0.35 (40 - 11.7)/80)	0.29 (11.7/40)
δ_p [dB]	0.01	0.01
A_s [dB]	32 ($\delta_s = 2.5 \cdot 10^{-2}$)	32 ($\delta_s = 2.5 \cdot 10^{-2}$)
FIR order	8	23
MAC/s [$\cdot 10^6$]	360	960

Table 4.2: Proposed HiperLAN/2 filter and decimate system performance



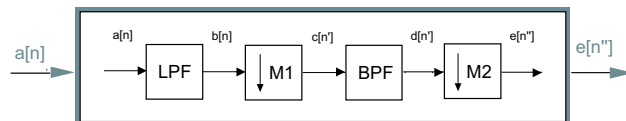
(a) Pre filter



(b) Post filter

Figure 4.11: Proposed HiperLAN/2 channel selection filters

-8 to 8 MHz. In that case the selection of channels at $f_c = 8.5$ and 9.5 would become impossible. So by using $M1 = 4$ and $M2 = 2$ all incoming channels can be adequately filtered after the first decimation. The post filter will be operating at the lower rate $f_{filter} = f_{AD}/M1$ and subsequent decimation will reduce the amount of filter operations by a factor $M2$. The proposed filter structure for the Bluetooth **ASAP** model is therefore that of figure 4.12. The low-pass filter acts as an anti-alias filter and the band-pass filter does the sharp channel selection at the lower rate. Polyphase implementation reduces filter operations of both filters. Estimates for

Figure 4.12: Filter and decimate proposal for Bluetooth **ASAP** model

the required filters⁷ of both filters is shown in table 4.3. The constraints on the anti-alias filter LPF have been reduced because the 7th order Butterworth filter in the analog front-end already attenuates signals $> 10MHz$. The thermal noise in the system is assumed to be in the order of -37 dB and can be permitted to fold back into the pass-band once. This increases the allowable transition bandwidth to $f_s = 20$ MHz. The stop-band attenuation is chosen to equal the required SNR for one Bluetooth channel. The required BPF filter order is quite large, but the low operating rate of the filter reduces the PF considerably. The total required MMAC/s is $170 + 895 = 1065$. This PF is $\approx 3/4$ of the HiperLAN/2 system PF, but this is mainly because for HiperLAN/2 two signal paths are filtered.

⁷The estimated filter orders are obtained by using Matlabs filter design and analysis (FDA) tool

Parameter	LPF	BPF
$\Omega_{p,s} (f/f_{filter})$	0.25 (10/40),0.5 (20)/40)	0.18 (1.8/10),0.22 (2.2/10)
$\Omega_{s,p} (f/f_{filter})$	-	0.28 (2.8/10),0.32 (3.2/10)
δ_p [dB]	0.01	0.01
A_s [dB]	21 ($\delta_s = 8.9 \cdot 10^{-2}$)	64 ($\delta_s = 6.3 \cdot 10^{-4}$)
FIR order	16	178
MAC/s [$\cdot 10^6$]	170	895

Table 4.3: Proposed Bluetooth filter and decimate system performance

4.2.7 Complex filters

Complex filters enable the system to reject signals at $f_{interference}$ while preserving a wanted signal at $f_{signal} = -f_{interference}$. This type of filter is suitable for the **ALAP** filter and decimate section. Complex filtering use two real filters for each input signal. By first comparison to the **ASAP** filter and decimate section, a complex filter system roughly increases the total amount of filter operations by a factor 4 (as shown in figure 4.13). However, anti-alias filtering before decimation by $M1 = 4$ does not require complex filters. The filter operations of the anti-alias LPF filter thus increases by a factor 2. For the full-complex BPF filters, methods are known for optimization. In [20] a complex FIR filter implementation is discussed using only three multipliers and two adders. Based on this information, performance

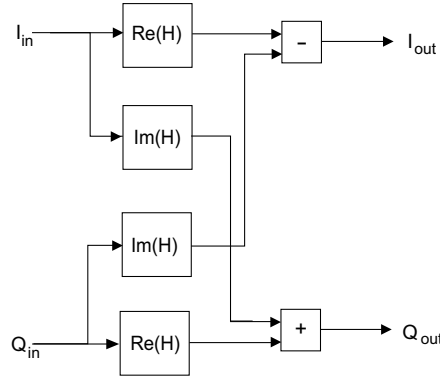


Figure 4.13: Complex filter structure [13]

figures for the **ALAP** filter and decimate block can be extrapolated from table 4.3. Roughly two real LPFs and three real BPFs are needed, resulting in a total PF of $2 \cdot 170 + 3 \cdot 895 = 3025$ MMAC/s. So far, **ALAP** requires roughly 3 times the processing required by **ASAP**. The comparison is not completely fair, because the Hilbert transformer and the post mixer filter of the **ASAP** system have not been added yet. The system comparison in chapter 6 will reveal the true performance champion.

4.3 CIC

Cascaded Integrator-Comb (CIC) [24],[3],[13] filters⁸ are multiplier-less structures, consisting of only adders, subtractors and registers. Multiplier-less structures are

⁸CIC filters are also known as *Hogenuer* filters.

usually very power efficient compared to regular structures. CIC filters are generally applied when large rate changes are needed. This is related to its pass-band characteristics which will be discussed in a moment. The two basic building blocks of a CIC filter are an integrator and a comb. An integrator is a single pole IIR filter with a unity feedback coefficient (eq 4.16).

$$y[n] = y[n - 1] + x[n] \Leftrightarrow H_I(z) = \frac{1}{1 - z^{-1}} \quad (4.16)$$

A Comb filter, running at the high sampling rate with a rate change of M is an odd-symmetric FIR filter described by eq. 4.17.

$$y[n] = x[n] - x[n - MD] \Leftrightarrow H_C(z) = 1 - z^{-MD} \quad (4.17)$$

D is a design parameter called the *differential delay* and can be any positive integer (but is usually limited to 1 or 2). An N stage CIC filter combines N integrator and N comb stages to an efficient structure with system transfer function (eq. 4.18).

$$H(z) = H_I^N(z)H_C^N(z) = \frac{(1 - z^{-MD})^N}{(1 - z^{-1})^N} = \left(\sum_{k=0}^{DM-1} z^{-k} \right)^N \quad (4.18)$$

The composite CIC filter is thus equivalent to a cascade of N uniform FIR filter stages with unit coefficients, in other words: a cascade of N boxcar filters. The frequency response has a low-pass characteristic. It can be obtained by evaluating eq. 4.18 at $z = e^{j\frac{2\pi f}{R}}$, where F is the frequency relative to the low sampling rate $f_{out} = f_{in}/M$ (eq. 4.19).

$$|H(f)| = \left| \frac{\sin(\pi Df)}{\sin(\frac{\pi f}{R})} \right|^N \approx \left| MD \frac{\sin(\pi Df)}{\pi Df} \right|^N \quad \text{for } 0 \leq f \leq \frac{1}{D} \quad (4.19)$$

A single stage implementation example of a CIC filter is shown in figure 4.14. In the design process M, D and N are chosen to provide acceptable pass-band

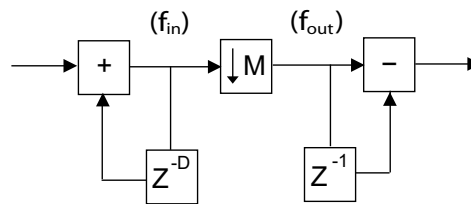


Figure 4.14: Single stage CIC filter implementation

characteristics. This ranges over the frequencies from zero to a predetermined cutoff frequency f_{cutoff} , expressed relative to the low sampling rate. Frequency bands that will alias back into the filter pass-band are given in eq. 4.20.

$$\frac{k}{D} \pm f_c \quad \text{where } k = 1, 2, \dots, \lfloor M/2 \rfloor \quad (4.20)$$

The phase response is linear in the pass-band, and the design parameters controlling the magnitude response are demonstrated in figure 4.15(a) (b) and (c). The input frequency $f_{in} = 80$ MHz for all plots. In figure 4.15(a), the decimation factor $M = 4$ and differential delay $D = 2$. It is clear that at least a 3 stage CIC is necessary to provide sufficient attenuation. This is necessary to prevent signals aliasing back into

the pass-band. In figure 4.15(b) the cut-off frequency of the pass-band is adjusted by the differential delay D . In figure 4.15(c) the decimation factor is changed. In case of Bluetooth channel selection of a carrier at $f_c = 0.5$ MHz, these parameters are sufficient to tailor the response to replace that of the low-pass pre-filter discussed in section 4.2.5. But for higher carrier frequencies the channels will be attenuated by the filter. None of the parameters discussed improve the pass-band characteristics enough to make this filter a feasible alternative that fits in the filter configuration of figure 4.12. For HiperLAN/2 channel selection (relatively wide channels) usage of this filter would require additional equalization, and the stop-band attenuation is very poor which introduces significant aliasing.

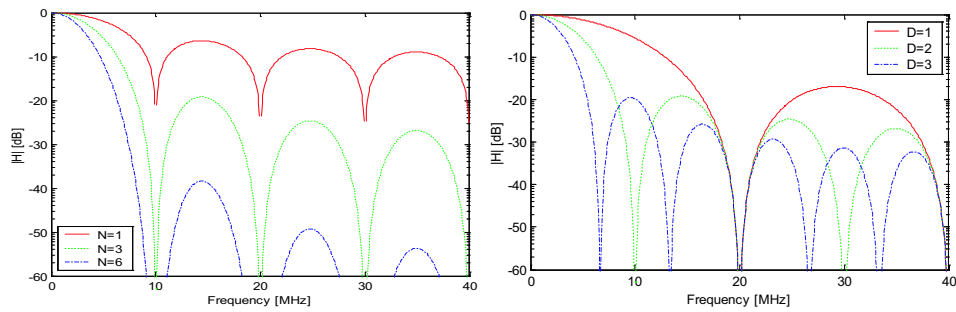
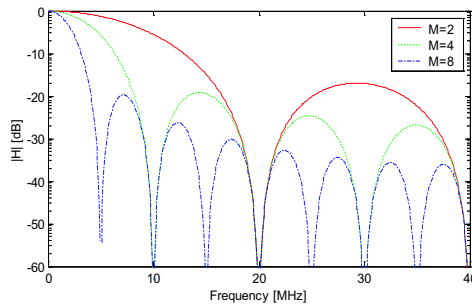
(a) Varying stages N ($D = 2, M = 4$)(b) Varying delay D ($N = 3, M = 4$)(c) Varying rate change M ($D = 2, N = 3$)

Figure 4.15: CIC Magnitude responses

4.4 IIR

IIR filters have several undesirable characteristics such as non-linear phase, sensitivity to coefficient quantization and complexity of design and analysis [21],[19],[18]. On the other hand, the amount of multiplications needed to perform filter operations is low compared to comparable FIR designs. Implementations of IIR filter structures are known that will inhibit them from instability [1]. The proposed HiperLAN/2 system of figure 4.7(c) requires a relatively small amount of filter operations if polyphase implementations are applied. The sensitivity of the HiperLAN/2 demodulator can not be tested at this time because it is still under development. This section will therefore focus on Bluetooth channel selection filters. A test environment will be used which includes a Bluetooth demodulator to investigate the sensitivity of the demodulator to non-linear phase response of some IIR filters.

4.4.1 Bilinear transform

A classic analog filter model can be mapped into a digital IIR using for instance the bilinear z -transform or the *impulse invariant* method. The latter guarantees that the impulse response of the digital transfer function is the same as that of the analog filter. The frequency response however can vary somewhat, favoring the bilinear transform method. Here, the analog Laplace operator s is substituted by its digital counterpart z as follows [21],[19]:

$$s = \frac{1 - z^{-1}}{1 + z^{-1}} \quad (4.21)$$

The $j\omega$ axis of the s -plane is mapped into the unit circle in the z -plane. The left half of the s -plane maps into the region *within* the unit circle (resulting in a *stable* system). The right half maps into the region *outside* the unit circle, representing an *unstable* system. Sometimes pre-warping is required to obtain the desired cut-off frequency in the digital domain .

4.4.2 Group delay

The phase response of a digital filter $\theta(\Omega)$ is obtained by taking the argument of it's transfer function. To find the *linear-ness* of this response the (frequency) derivative is taken. The function is the measure for phase non-linearity and called the *Group delay* τ :

$$\tau(\Omega) = \frac{d\theta}{d\Omega} \quad (4.22)$$

For FIR filters this value is a constant, i.e. every spectral component of the input signal is delayed τ seconds. The frequency dependent variations in group delay for IIR filters is different for several design methods. It can be seen as a design parameter and traded off against for instance transition band width. For instance an elliptic filter has very steep transitions, resulting in higher group delays. The Butterworth and Chebyshev Type II filters typically have low group delay, and this causes broader transition bands and stop-band ripples.

4.4.3 Filter types

Butterworth

A well known filter design method in the analog world can be used in the digital domain as well using (for instance) the bilinear transform. The pass-band is maximally flat and the stop-band attenuation is well over 30 dB. The required filter

order is 28. The magnitude response is given by:

$$|H(\Omega)|^2 = \frac{1}{1 + (\Omega)^{2N}} \quad (4.23)$$

The poles are thus distributed along a circular arc at locations separated by π/N radians.

Chebyshev

Chebyshev filters typically have narrower transition band widths compared to Butterworth filters. The penalty for this steeper transition is phase non-linearity. There are two types of filters based on the following Chebyshev polynomial:

$$Ch_N(\omega) = \cos(N \cos(\omega)) \quad (4.24)$$

The first type (I) has a ripple in the pass-band and is smooth in the stop-band. The squared magnitude response is given by:

$$|H(\Omega)|^2 = \frac{1}{1 + \varepsilon^2 Ch_N^2(\Omega)} \quad (4.25)$$

If maximal flatness is desired in the pass-band, this can be done at the expense of ripples in the stop-band. Now, the squared magnitude response is given by:

$$|H(\Omega)|^2 = \frac{1}{1 + \frac{1}{\varepsilon^2 Ch_N^2(\Omega)}} \quad (4.26)$$

This is called a Chebyshev Type II filter. Both types of filter meet specifications with a minimal order of 12.

Elliptic

Elliptic or *Cauer* filters have both equiripple pass- and stop-bands and a very narrow transition band. The phase is (therefore) highly nonlinear. The specified transition band width is met with $N=8$.

All-pass correction filters

A technique that can be applied to reduce the non-linearities of IIR filter phase responses is the application of (all-pass) correction filters⁹ [18]. A filter can be designed to have arbitrary phase response and unity magnitude response. If used in cascade with an IIR filter, the total phase response can be designed to be more linear. The size of the all-pass correction filter must be equal to that of the filter it is cascaded with. Thus, the feasibility of this method is questionable and depends on the sensitivity of the demodulator to non-linear phase response.

Fixed point stability

The IIR filters that are used for this model were designed using the MATLAB filter design and analysis toolbox. The filter transfer functions that have been used are stable for 16 bit fixed point implementations. They can be implemented using second order sections that will inhibit them from erratic behavior. The functional tests however were conducted using floating point arithmetic for maximum flexibility. The actual implementation of the proposed IIR filters is recommended for further studies.

⁹All-pass correction filters are also known as *phase equalizers*

Input	f_c [MHz]	2.5
	Rate [Ms/s]	80
	Noise [dB]	-13
	Time [s]	0.1
Decimation	$M = M1 \cdot M2$	$8 = 4 \cdot 2$
FIR	Type	Remez
	Order	85
	$\Omega_{s,p}$ [rad/s]	[0.18,0.20]
	$\Omega_{p,s}$ [rad/s]	[0.30,0.32]
	δ_p [dB]	0.690
	A_s [dB]	-21
	BER	0.0237
FIR	Type	Remez
	Order	55
	$\Omega_{s,p}$ [rad/s]	[0.18,0.20]
	$\Omega_{p,s}$ [rad/s]	[0.30,0.32]
	δ_p [dB]	1.175
	A_s [dB]	-17
	BER	0.0658

Table 4.4: IIR test configuration

4.4.4 Demodulator sensitivity tests

This section will do a quantitative analysis of the Bluetooth demodulators sensitivity to non-linear phase response of the BPF channel selection filter(s). The references will be two equiripple FIR filters of different order. The pass-band ripples of both prototype filters are significantly larger than the previously assumed $\delta_p = 0.01$. The tolerance region of this parameter for practical filters (i.e. lowest possible order) appears to be around 1 dB for FIR filters. Furthermore, the filter specifications are based on the band-pass requirements of section 3.4 after minor adjustments to compensate for transition band-widths of the applied filters. The filter and decimate system that is used is based on the system of figure 4.12 on page 35. Thus, no Hilbert transform is applied and only real signals are present at the input. Furthermore, the anti-alias LPF filter is left out to make sure the only filter influence on the signal is done by the test filter. The Simulink model used for testing is shown in figure 4.16. The BPF is implemented by using a FIR, IIR and IIR followed by an all-pass correction (APC) filter. The same input signal is thus filtered with 3 different alternatives for implementing the BPF filter and demodulated separately. After demodulation, BER calculations are done to measure their performance. The FIR block was tested with two equiripple prototypes of different order, with design parameters as shown in table 4.4. Since there are no strong adjacent interferences, filter orders have been chosen to produce similar results for comparison. The wanted channel has a carrier frequency of $f_c = f_{demod} = 2.5$ MHz. The noise level is arbitrary and chosen to cause sufficient bit errors for reliable BER calculation in the available simulation time. The group delay of the IIR filters has peaks in the transition region. Several tests are done with different pass-band widths to test the sensitivity of the demodulator from a spectral location point of view. In other words: how does the spectral location of the phase distortion influence the BER.

Elliptic filter

The Elliptic filter has a high degree of phase non-linearity and narrow transition band. The filter order is chosen to be $N = 6$, resulting in 13 filter coefficients in

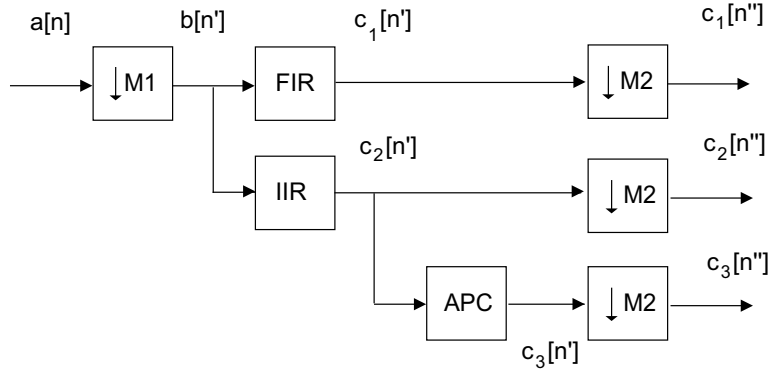
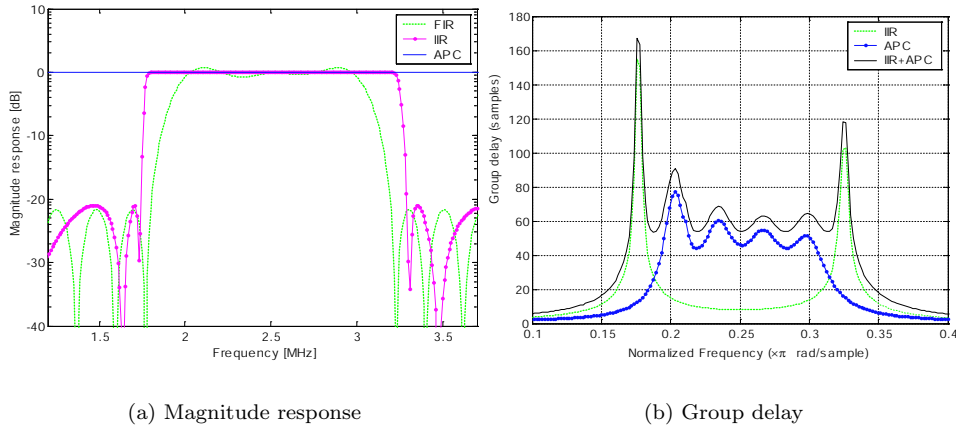


Figure 4.16: Bluetooth: IIR band-pass filter test

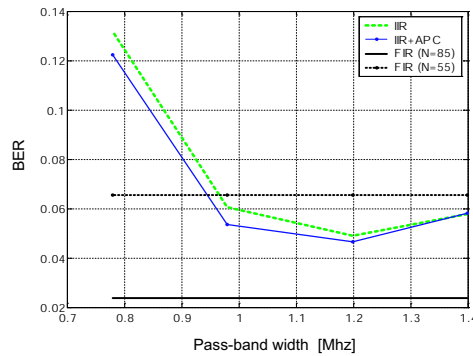
both the numerator and denominator of the transfer function. The group delay characteristics for the filter with $\Omega_{1,2} = [0.18, 0.32]$ compared to the prototype FIR is shown in figure 4.17(a). The magnitude of the pass-band is very flat compared to the FIR filter, and the stop-band response is comparable. From the group delay

Figure 4.17: Elliptic filter comparison, $\Omega_{1,2} = [0.18, 0.32]$, $N = 6$

plot (shown in figure ??(b)) it is clear that the phase is highly nonlinear around the cut-off frequencies. The all-pass correction filter therefore delays the spectral components in the pass-band, equalizing the group delay. The results in table ??(a) and figure (b) show the bad performance of the IIR filter and the minimal improvements by applying the correction filter. Apparently, the correction filter imposed group delay has too much ripple to significantly improve the linearity. The optimal pass-band width is 1.2 MHz. Referring to figure 4.17(b), the group delay without correction filter is quite flat from 0.2 to 0.3 $\pi rad/sample$. There is however a strange spike in the transition band region of $\Omega = 0.19$ which I cannot fully explain. An IIR filter with a better intrinsic phase linearity at the cost of transition band width is thus more likely to improve performance. Furthermore, a FIR filter with $N = 55$ outperforms the IIR filter for narrow pass band widths. Judging from the large pass-band ripple of this FIR, the sensitivity to δ_p is smaller than sensitivity to linear phase.

$\omega_{s,p}$ [rad/s]	BW [MHz]	BER IIR	BER IIR+APC
[0.180, 0.320]	1.40	0.0576	0,0579
[0.190, 0.310]	1.20	0.0491	0,0464
[0.201, 0.299]	0.98	0.0606	0,0534
[0.211, 0.289]	0.78	0.1317	0,1222

(a) BER results table

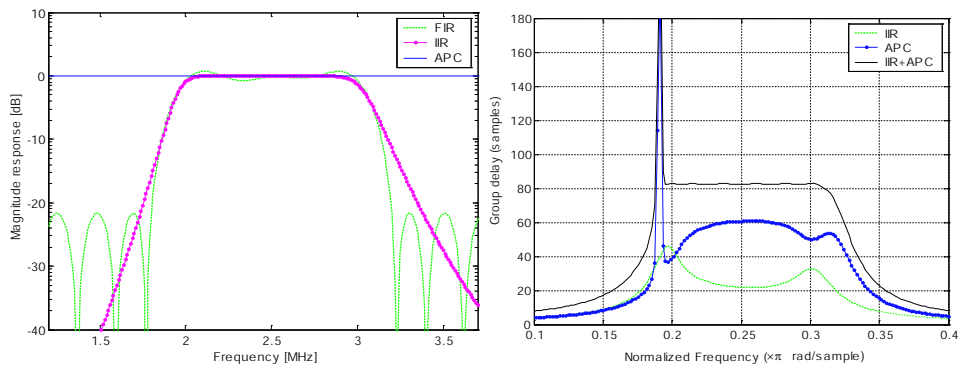


(b) BER results plot

Figure 4.18: Elliptic IIR (with and without APC, $N = 6$) BER vs BW

Butterworth filter

The Butterworth filter has a lower degree of phase non-linearity compared to other IIR filters. Again, the filter order is chosen to be $N = 6$ for a fair comparison. The group delay characteristics for the filter with $\omega_{1,2} = [0.195, 0.305]$ compared to the prototype FIR is shown in figure 4.19(a). Again, the magnitude response in the pass-band is very flat compared to the FIR filter. The transition band width of the Butterworth filter is slightly wider, the stop-band attenuation is larger. After the



(a) Magnitude response

(b) Group delay

Figure 4.19: Butterworth filter comparison, $\omega_{1,2} = [0.195, 0.305]$, $N = 6$

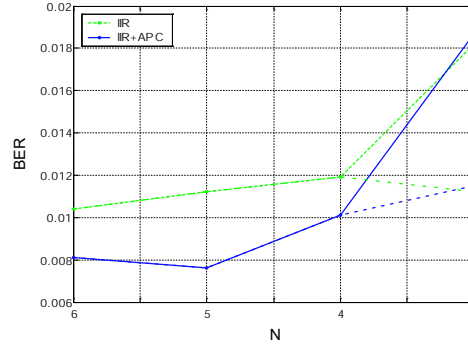
Parameter	LPF (FIR)	BPF (FIR)
$\Omega_{p,s}$	0.25 (10/40),0.5 (20)/40)	0.18 (1.8/10),0.22 (2.2/10)
$\Omega_{s,p}$	-	0.28 (2.8/10),0.32 (3.2/10)
δ_p [dB]	1	1
A_s [dB]	21 ($\delta_s = 8.9 \cdot 10^{-2}$)	64 ($\delta_s = 6.3 \cdot 10^{-4}$)
Filter order	16	104
MAC/s [$\cdot 10^6$]	160	520

Table 4.5: Bluetooth FIR filter and decimate system performance

first simulation it is already clear that this filter is much more suitable than the Elliptic filter. Without correction filter, it outperforms the 85th order FIR prototype by reducing the BER by 50%. With this headroom, the following simulations are done decreasing the IIR filter order. Table 4.20(a)¹⁰ and figure (b) reveal the

N	BER IIR	BER IIR+APC
6	0,0104	0,0081
5	0,0112	0,0076
4	0,0119	0,0101
3	0,0182	0,0187
3*	0,0112	0,0115

(a) BER results table



(b) BER results plot

Figure 4.20: Butterworth IIR (with and without APC, $N = 6$) BER vs BW

power of the IIR Butterworth filter. Even with the lowest order $N = 3$ the BER is better than the FIR prototype. The reduction in filter coefficients also reduces phase non-linearity while stop-band attenuation remains good. The transition bandwidth increased beyond the optimum, resulting in a redesign of the filter (denoted by a (*) in the table) to regain performance. Again the all-pass correction filter improvements do not justify its application.

Bluetooth filter and decimate (Mixed FIR-IIR)

Based on the previous results, the Butterworth IIR filter is a viable alternative for the FIR prototype. Extrapolating these results to equal the proposed system of section 10 yields table ???. The PF of the IIR filters needs more explanation. Assume an implementation as shown in figure 4.2(b) on page 24. The numerator of the LPF transfer function has 5 non-zero coefficients. This results in a $PF_{num} = 5 \cdot 80 \cdot 10^6 = 400$ GMAC/s. The denominator has 5 non-zero coefficients, of which one is 1. This results in a $PF_{den} = 4 \cdot 80 \cdot 10^6 = 320$ GMAC/s. The combined

¹⁰(*)To re-fit the magnitude response to the FIR prototype, the pass band width is reduced to $\omega_{1,2} = [0.201, 0.299]$

Parameter	LPF (IIR)	BPF (IIR)
$\Omega_{p,s}$	0.25 (10/40), 0.5 (20)/40)	0.18 (1.8/10), 0.22 (2.2/10)
$\Omega_{s,p}$	-	0.28 (2.8/10), 0.32 (3.2/10)
δ_p [dB]	1	1
A_s [dB]	21	32
Filter order	4	12
MAC/s [$\cdot 10^6$]	180	190

Table 4.6: Bluetooth IIR filter and decimate system performance

$PF_{LPF} = PF_{num} + PF_{den} = 720$ GMAC/s. Polyphase implementation taking advantage of $M1 = 4$ reduces this by a factor 4. The numerator of the BPF transfer function has 13 coefficients, of which 7 are non-zero. This results in a $PF_{num} = 7 \cdot 20 \cdot 10^6 = 140$ GMAC/s. The denominator has 13 non-zero coefficients, of which one is 1. This results in a $PF_{den} = 12 \cdot 20 \cdot 10^6 = 240$ GMAC/s. The combined $PF_{IIR} = PF_{num} + PF_{den} = 380$ GMAC/s. Polyphase implementation taking advantage of $M2 = 2$ reduces this by a factor 2. Thus, the filter operations of the BPF are significantly reduced if an IIR Butterworth filter is used. For the LPF implementation a FIR filter is preferred due to the better PF.

4.4.5 Conclusions

HiperLAN/2

With the known parameters for HiperLAN/2, the optimal decimation factor M has been calculated for a 2 filter system. The proposed system is depicted in figure 4.7(c). A FIR only implementation is targeted because the demodulator is not available for (IIR) phase (non-)linearity tests. The required filter operations based on theoretical (filter) specifications (as described in section 2.4) are as listed in table 4.2. The total PF estimate of the HiperLAN/2 filter and decimate system is thus $360 + 960 = 1320$ MMAC/s.

Bluetooth

For Bluetooth, the design procedure was a little more complicated than for HiperLAN/2. The proposed **ASAP** filter structure of figure 4.12 was derived and a FIR-only and combined IIR-only implementation were analyzed. Based on these results, a mixed FIR-IIR filter and decimate system is proposed. The PF estimate of this system can be obtained by adding the PF of the FIR LPF of table 4.5 and IIR BPF of table 4.6: $160 + 190 = 350$ MMAC/s. Extrapolating again, the **ALAP** filter structure will require roughly $2 \cdot 160 + 3 \cdot 190 = 890$ MMAC/s. The performance gap is closing and the duel between **ASAP** and **ALAP** will become even closer in chapter 6. In the next chapter the frequency translation block is discussed, which is also followed by a band-pass filter. The specifications of this filter will also be derived.

5

Digital Mixer

5.1 Introduction

This chapter will go into the consequences of frequency translation. In general, a mixer implementation can be either real, half-complex or complex. One way of implementing a half-complex mixer was already discussed in section 3.2. For the **ASAP** system (shown in figure 3.6 on page 18) this method can also be used, or a real mixer can be applied. The **ALAP** system (depicted in figure 3.7 on page 19) would be best served by a full complex mixer. An overview of the pro's and con's of these filter types will be discussed followed by methods to implement such a mixer. Then, specific design choices are made concerning the layout of the frequency translation block of the proposed Bluetooth channel selection system.

5.2 Real Mixer

A real bandpass signal with carrier frequency f_c , multiplied by a harmonic wave with frequency f_{lo} produces sum- and difference spectra at $f_{lo} + f_c$, $f_{lo} - f_c$, $-(f_{lo} + f_c)$ and $-(f_{lo} - f_c)$. The functional block performing this operation is called a *real mixer*. In figure 5.1 the incoming signal $x(nT)$ is centered at $f_c = 0.5$ MHz. The positive spectrum of the real signal is black and the negative spectrum is white. The real mixer is implemented as a cosine generator with $f_{lo} = 2$ MHz (white) and mirror frequency in black (at $-f_{lo} = -2$ MHz). The resulting spectra are thus located at -2.5 , -1.5 , 1.5 and 2.5 MHz. The spectra at -1.5 and 1.5 MHz are unwanted requires additional filtering to be removed.

5.3 Hilbert-mixer

The Hilbert transformation (refer to section B was discussed in it's FIR filter implementation form. It can also be implemented by using a pair of local oscillators. The 90 degree phase difference is realized by multiplying the I path with a cosine and Q with a sine wave. This results in a double *real mixer* structure shown in figure 5.2. By adding or subtracting both paths afterwards the positive or negative spectrum is chosen and I and Q are combined to form a real band-bass signal.

5.4 Required mixer frequencies

The mixer frequency depends on the selected channel carrier frequency f_c and the required demodulator frequency f_{demod} . Based on the decimation factor considera-

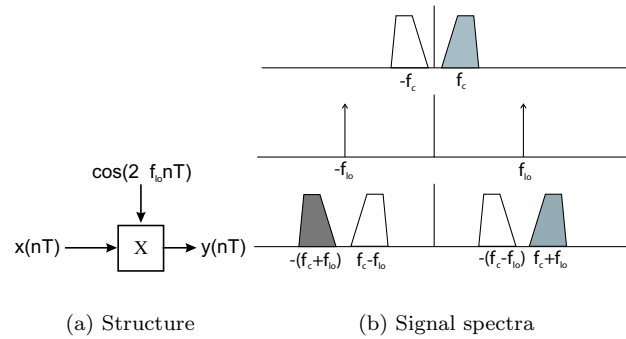


Figure 5.1: Real mixer (real input and injection)

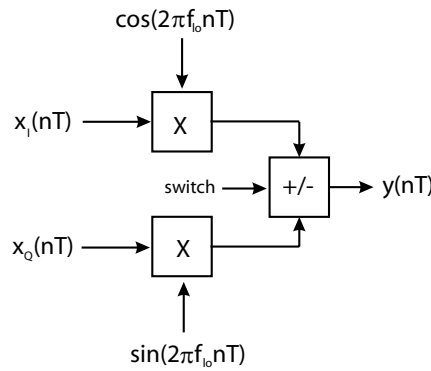


Figure 5.2: Double real mixer (Hilbert transform)

tions of section 10 the demodulator requires the channel at $f_{demod} = 2.5$ MHz. After channel selection filtering and the subsequent decimation, all selected channels are between -5 and 5 MHz due to aliasing. This was shown using frequency spectra in figure 4.5 of section 4.2.5. If the operation is viewed in the time domain it becomes even more clear. In figure 5.3 a channel with $f_c = 7.5$ MHz is shown before (a) and after decimation by $M2 = 2$ (b). Based on this theory only two oscillator frequencies are required to mix all possible carriers to f_{demod} , as shown in table 5.1. The first column is the original carrier frequency f_c and the second column the aliased frequency f'_c . Column three lists the oscillator frequency required to mix the carrier to f_{demod} and either column four or five shows the unwanted images that have to be filtered out afterwards.

5.5 Conclusions

For both **ASAP** and **ALAP** systems real mixers are proposed. (Half-) complex mixers have complex outputs that require an additional Hilbert transformer to convert the signals to real signals. For the **ALAP** system a double real mixer with 90 degrees out of phase oscillators is proposed. This will be referred to as the Hilbert-mixer. Due to decimation it is possible to translate all carrier frequencies to the required f_{demod} with only two oscillator frequencies. This makes the use of IIR oscillators more feasible [13].

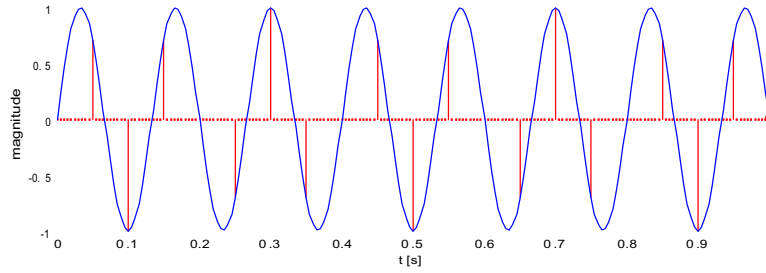
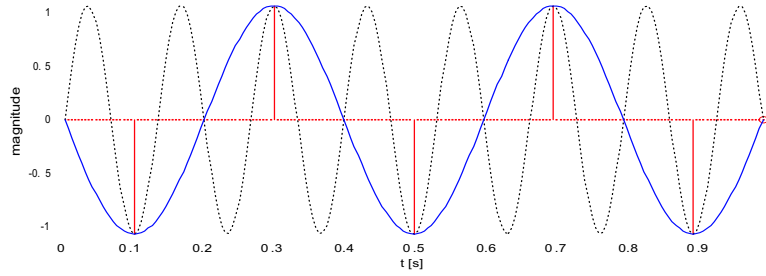
(a) $f_c = 7.5$, $f_s = 20$ MHz(b) $f'_c = 2.5$, $f_s = 10$ MHz

Figure 5.3: Aliasing due to sub-sampling

f_c [MHz]	f'_c [MHz]	f_{lo} [MHz]	$f'_c - f_{lo}$ [MHz]	$f'_c + f_{lo}$ [MHz]
0.5	0.5	2.0	-1.5 (1.5)	2.5
1.5	1.5	1.0	0.5	2.5
2.5	2.5	-	2.5	2.5
3.5	3.5	1.0	2.5	4.5
4.5	4.5	2.0	2.5	6.5 (1.5)
5.5	4.5	2.0	2.5	6.5 (1.5)
6.5	3.5	1.0	2.5	4.5
7.5	2.5	-	2.5	2.5
8.5	1.5	1.0	0.5	2.5
9.5	0.5	2.0	-1.5 (1.5)	2.5

Table 5.1: Mixer frequencies for $f_{demod} = 2.5$ MHz

6

System

6.1 Introduction

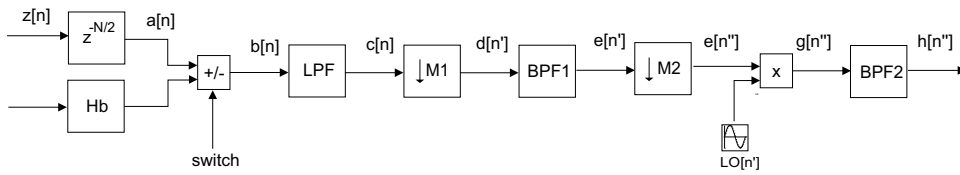
In the previous chapters most of the channel selection sub-systems were researched and defined. For HiperLAN/2 the currently proposed system is somewhat immature. A FIR-only implementation was derived in section 4.2.5. Due to the late availability of the demodulator further evolution of the model remains work for the future. A first model and test run of the HiperLAN/2 channel selection, based on the early designs of 3.4 was carried out in [5]. For Bluetooth, two systems are proposed: **ASAP** and **ALAP**. These are shown in figure 6.1. Note that for convenience some optimizations are not explicitly modelled. These include the polyphase implementation and the 3 multiplier, 2 adder implementation of the complex BPF filter (in the **ALAP** system, see section 4.2.7). After a description of the test environment and the BER tests that will be conducted the proposed systems will be examined.

6.2 Test environment and parameters

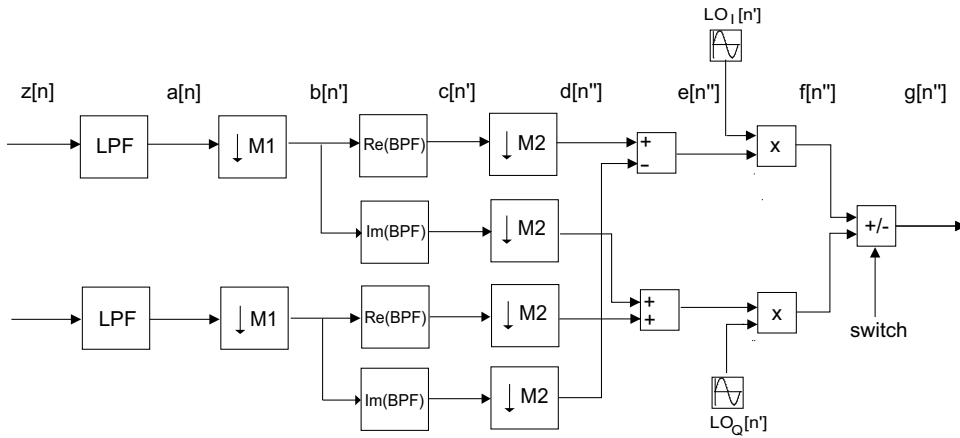
To test the proposed channel selection system a modulator and demodulator are added to the system. The signal generation blocks and the analog front-end are shown in figure 6.2. The output signals $z_i[n], z_Q[n]$ are the inputs to the channel selection system. Channel and interfering signals are generated by using a baseband Bluetooth signal generator and the noise is bandlimited. The baseband channel and interferer are mixed to a "RF" frequency of 100 MHz. The actual RF frequencies in the 2.4 GHz band are not used as this would needlessly increase simulation times. The composite signal is called $x(t)$. The analog front-end is simulated with a quadrature down-mixer and analog low-pass filter (LPF_A), followed by a zero-order-hold (ZOH) block. The ZOH block represents the AD converter and from that point, the signals are considered digital (as shown in figure 6.2). The parameters used that are not part of the ASAP system are listed in table 6.1. The interference signal strengths are relative to that of the selected channel (and thus indicated by a +/- sign).

6.2.1 BER tests

The behavior of the system will be analyzed using the signals listed in table 6.2. With these signals, four combinations per channel selection system must be processed and a minimum BER of 0.1% must be achieved (without error correction).



(a) **ASAP** system



(b) **ALAP** system

Figure 6.1: Bluetooth channel selection

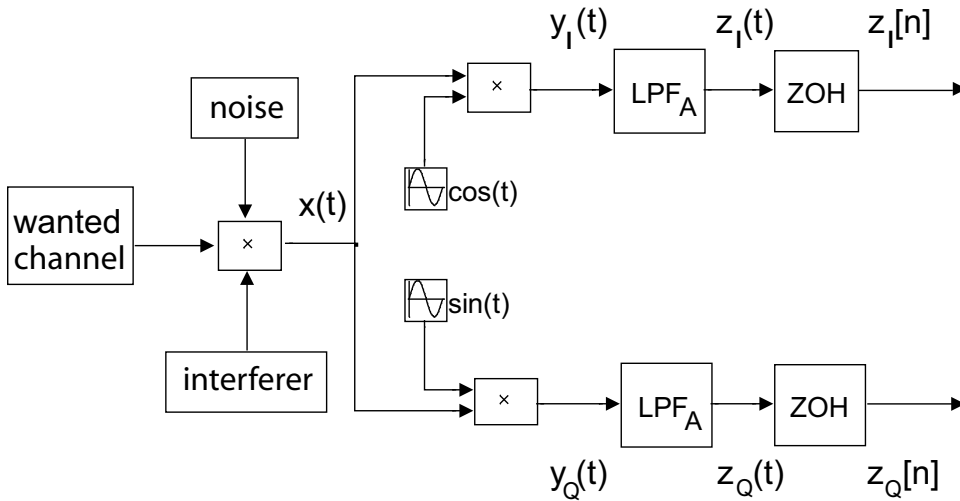


Figure 6.2: Simulink model of test environment

This results in the four tests that will be referred to as BER test 1,2,3 and 4. The input signal $x(t)$ for these test are listed below:

1. Selected channel + Noise + Co-channel interfeerer

Function	Parameter	Value
Channels and interferers	RF Frequency [MHz]	$90 \leq f_{c,RF} \leq 110$
	IF Frequency [MHz]	$-10 \leq f_{c,IF} \leq 10$
Selected channel	Strength [dB]	0
Co-channel interferer	Strength [dB]	-11
Adjacent channel interference ≥ 1 MHz	Strength [dB]	0
Adjacent channel interference ≥ 2 MHz	Strength [dB]	+30
Adjacent channel interference ≥ 3 MHz	Strength [dB]	+40
Noise (bandwidth 400 MHz)	Strength [dB]	-37
Local oscillator (analog)	Frequency [MHz]	100
Low-pass filter (analog)	Type	Butterworth
	Order	7
	Cut-off frequency [MHz]	10
Zero-order-hold	Frequency [MHz]	80
Demodulator (Bluetooth)	Input rate [MHz]	10
	Samples per symbol	10
	f_{demod} [Mhz]	2.5

Table 6.1: Parameters of the channel selection test environment

2. Selected channel + Noise + Adjacent channel interference ≥ 1 MHz
3. Selected channel + Noise + Adjacent channel interference ≥ 2 MHz
4. Selected channel + Noise + Adjacent channel interference ≥ 3 MHz

As these four input signals will be referenced a lot in the following sections, it is sometimes helpful to refer to them in a more descriptive manner. The experiment with the four aforementioned configurations of $x(t)$ will then be referred to as the *co-channel*, *adjacent 1*, *adjacent 2* and *adjacent 3* signals. The maximum duration of the BER tests that were done was 0.1 seconds. This is approximately 158 DH1 frames containing 216 bits each. The number of erroneous bits was thus divided by ≈ 34000 (the total amount of bits sent).

Signal	f_{IF} [MHz]	Strength [dB]
Selected channel	4.5	0
Co-channel interferer	4.5	-11
Adjacent channel interference ≥ 1 MHz	5.5	+0
Adjacent channel interference ≥ 2 MHz	6.5	+30
Adjacent channel interference ≥ 3 MHz	7.5	+40

Table 6.2: Wanted channel and interferer frequencies used for analysis

6.3 ASAP system 1

6.3.1 Introduction

The proposed demodulator system depicted in figure 6.1(a) contains two functional blocks that have not been designed yet. For the Hilbert transformer, this will be done in section 6.3.2. The post-mixer filter is designed in section 6.3.3. Then, the complete system is designed and can be tested following the BER tests specified in the Bluetooth specifications. Based on these simulations, the design space of the system will be explored and optimization paths pursued.

6.3.2 Hilbert transformer (Hb) design

The Hilbert transformer block is responsible for the 90 degree phase shift (-90° for $f \geq 0$ and $+90^\circ$ for $f \leq 0$) of the Q signal as described in Appendix B. In the ASAP system, this is done by a FIR filter implementation of the Hilbert transform. The ideal magnitude response of the Hilbert filter has a flat pass-band. In figure 6.3(a) the cancellation of the wave is demonstrated for an ideally flat magnitude response. The pass-band ripple δ_p of the practical Hilbert transformer distorts the amplitude of the wave and a residual signal remains. Even for small ripples in the pass-band, the residual signal of a 40 dB stronger adjacent carrier is still a strong interferer. Referring to section 4.2.4, stringent requirements on pass-band ripple can result in a large filter. The magnitude response of a FIR Hilbert implementation also

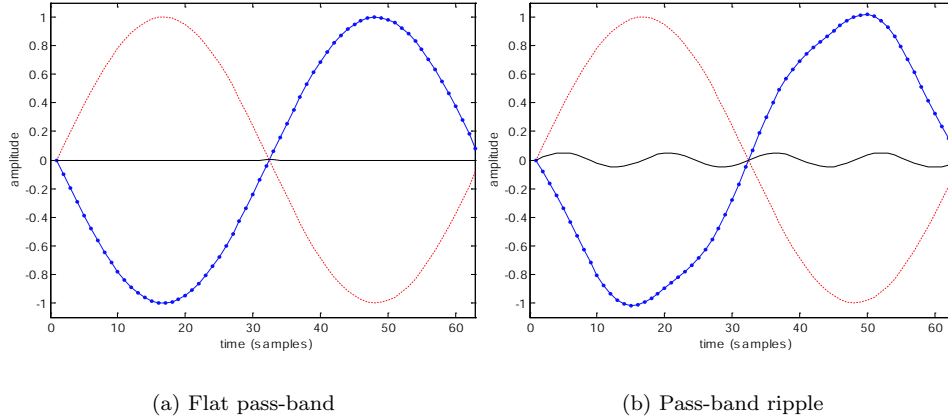


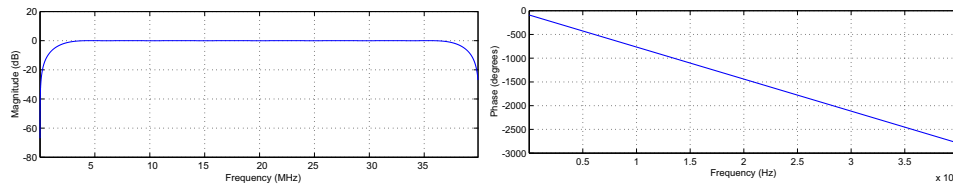
Figure 6.3: Influence of Hilbert transformer pass-band ripple

suffers from a finite transition band-width. This causes a rather poor response for the channel(s) close to baseband, as shown in figures 6.4(a) and (c). Experiments have shown that a minimal Hilbert filter order of $N = 49$ is required to sufficiently attenuate a 40 dB stronger interference at $-f_c$.

6.3.3 Post mixer filter (BPF2) design

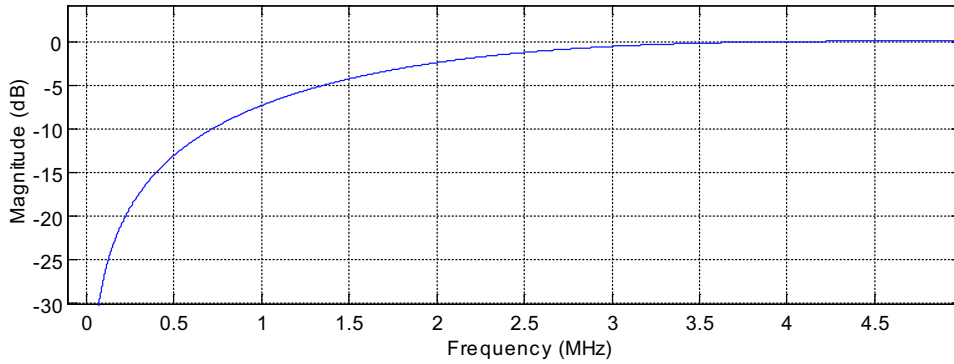
To remove the mixer products of the channel (and possible interferers) a second band-pass filter (BPF2) is required. By designing this filter, a second purpose can also be pursued: reducing the constraints on the first channel selection filter (BPF1). Thus, the required attenuation of BPF2 is determined by BPF1 and the required attenuation of the mixer products. The filtered signal $h[n'']$ is required to have a signal to noise ratio (SNR) of 21 dB [23]. Thus if the carrier frequency f_c of the selected channel is for instance $f_c = 0.5$ MHz the mixer product¹ at $f = f'_c - f_{lo} = 1.5$ MHz must be attenuated by at least 21 dB. In addition, strong interferers that have not been sufficiently attenuated by BPF1 must also be filtered out. Simulations are done to determine the trade-offs between the BPF1 and BPF2 filter requirements.

¹The local oscillator frequencies for frequency translation are listed in table 5.1



(a) Magnitude response

(b) Phase response



(c) Magnitude response (zoomed)

Figure 6.4: Hilbert transformer

6.3.4 Spectral analysis of the systems signals

Input to LPF: $b[n]$

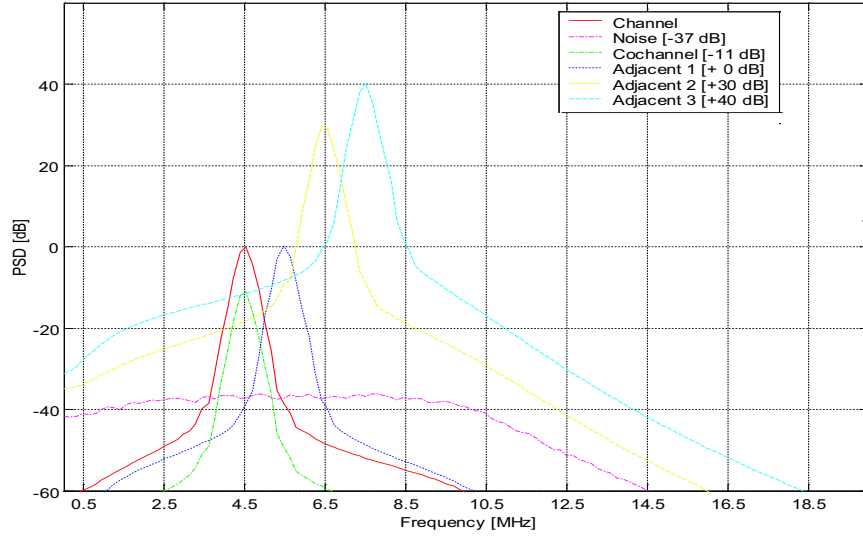
Now the signal spectra at the input of the channel selection system are examined and the effect of the filter and decimate operations. Referring to figure 6.1(a), $b[n]$ is the input for the low-pass filter. The four BER test signals are shown in the same figure. The effect of the analog LPF_A is best shown by the skirt of the strongest interferer. The right side is a lot steeper than the left side due to attenuation in the analog front-end.

Input to BPF1: $d[n']$

Most of the channel selectivity is provided by BPF1. Here, adjacent channel interferers must be sufficiently attenuated to prohibit unwanted images in-band after mixing. Furthermore, as the wanted channel is determined by frequency hopping, the filter coefficients must be updated every hop. So not only filter operations but also memory is saved with minimizing coefficients here. Using specifications from chapter 4, (refer to table 4.3 on page 36) a FIR filter of order 178 or an IIR filter of order 12 is necessary to achieve the specified BER. In figure 6.6 the 4 BER test signals are shown including a 104th order FIR BPF1 filter response. This attenuates the interferers over 53 dB.

Input to BPF2: $g[n'']$

After frequency translation, the signals are called $g[n'']$ and depending on the characteristics of BPF2 there can be quite some unwanted interference left. For the

Figure 6.5: Different LPF input signals $b[n]$

Signal	$f_c(f'_c)$ [MHz]	$f'_c - f_{lo}$ [MHz]	$f'_c + f_{lo}$ [MHz]
Selected channel	4.5	2.5	6.5 (3.5)
Co-channel interferer	4.5	2.5	6.5 (3.5)
Adjacent 1	5.5 (4.5)	2.5	6.5 (3.5)
Adjacent 2	6.5 (3.5)	1.5	5.5 (4.5)
Adjacent 3	7.5 (2.5)	0.5	4.5

Table 6.3: Mixed channel and interferer frequencies

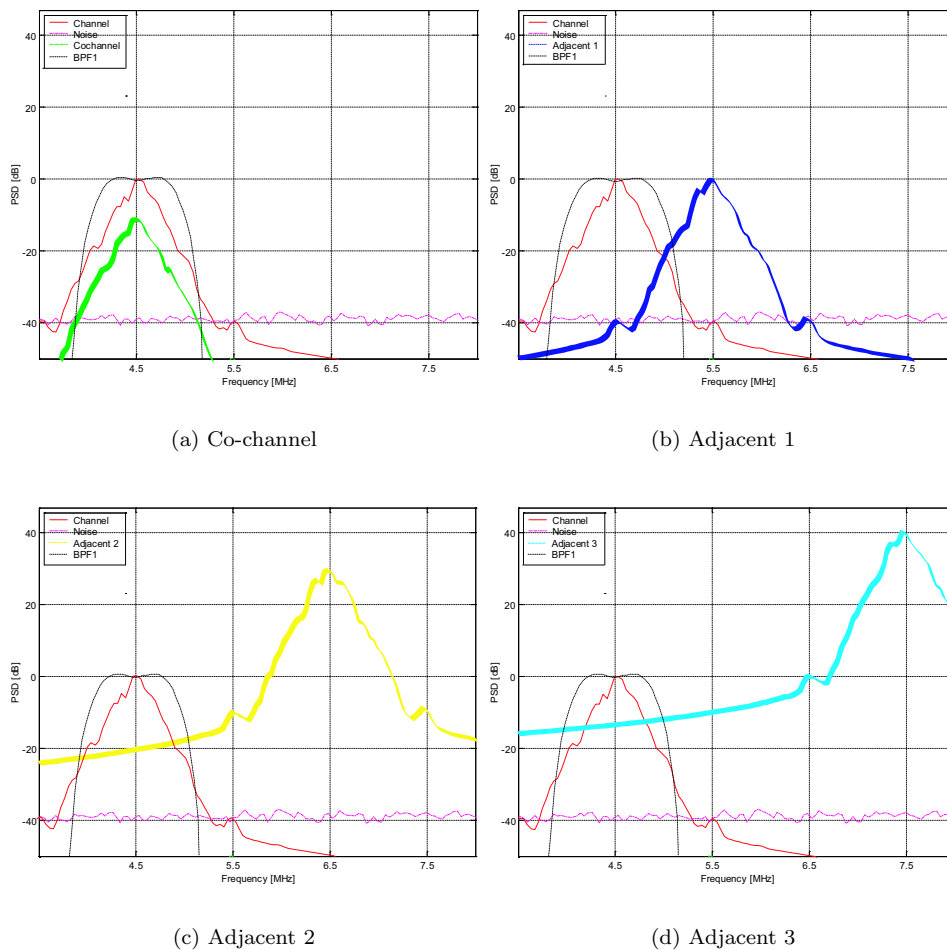
selected carrier and interferers, unwanted images (and aliases) occur at the frequencies listed in table 6.3. The first column already shows that BPF1 must attenuate adjacent 3 more than $40 + 11$ dB. If not, the signal becomes a co-channel interference of worse proportions than the specified worst-case co-channel interference ! The BPF2 filter must make sure that all interferences that are left (see figures 6.7) are attenuated by at least 21 dB². A 50th order Hamming window FIR filter was chosen for its good stop-band attenuation (keeps decreasing, as opposed to the flat equiripple stop-band).

Input to demodulator: $h[n'']$

When digital channel selection is completed the $h[n'']$ signal enters the demodulator. The demodulator performs frequency demodulation, produces bit error estimates and eye diagrams for diagnostic purposes. The eye diagram is used to judge the performance of the channel selection filters. If the SNR of the received signal is over 16 dB it is likely that the BER requirements will be met³. In figure 6.8 the output spectra of the selected channel and all 4 interferers are shown. Adjacent 1 and 2 seem to be of the least concern for this configuration. The question is whether eye diagrams and BER calculations agree.

²The reference sensitivity level of the Bluetooth demodulator is 21 dB [23]

³The demodulator used in the system was found to meet requirements with a SNR of 16 dB in a noise only environment[10]. This is 5 dB "better" than the required sensitivity

Figure 6.6: Transfer function of BPF1 and its incoming signal $d[n']$

6.3.5 Eye diagrams

For the signal spectra seen so far, eye diagrams are also included. Spectral analysis is a useful tool in for instance filter design, but not all necessary information is provided. The frequency demodulation scheme of the demodulator for instance is less sensitive to co-channel interference than to an equally strong interference in its "skirt". The information carried by the channel is in frequency variations, and thus the carrier frequency itself is of less importance. The eye diagrams corresponding to the signals from the current system as specified above are shown in figure 6.9. The eye diagram of (a) is too closed to achieve the specified bit error rate. How is this possible? All interfering signals are nicely filtered out and still a test fails! This shows the inverse relationship between extensive filtering and the open-ness of the eye diagram. By "shaving off" the (frequency) band edges the frequency modulated carrier loses information and is eventually reduced to a simple harmonic wave with frequency f_c ⁴. Thus, reducing the BER of test 1 will increase those of tests 2,3 and 4. A trade-off must be made between adjacent and co-channel interference. This leads to the conclusion that an optimal system is achieved when all eye diagrams

⁴Notice that this is exaggerated a little to make a point.

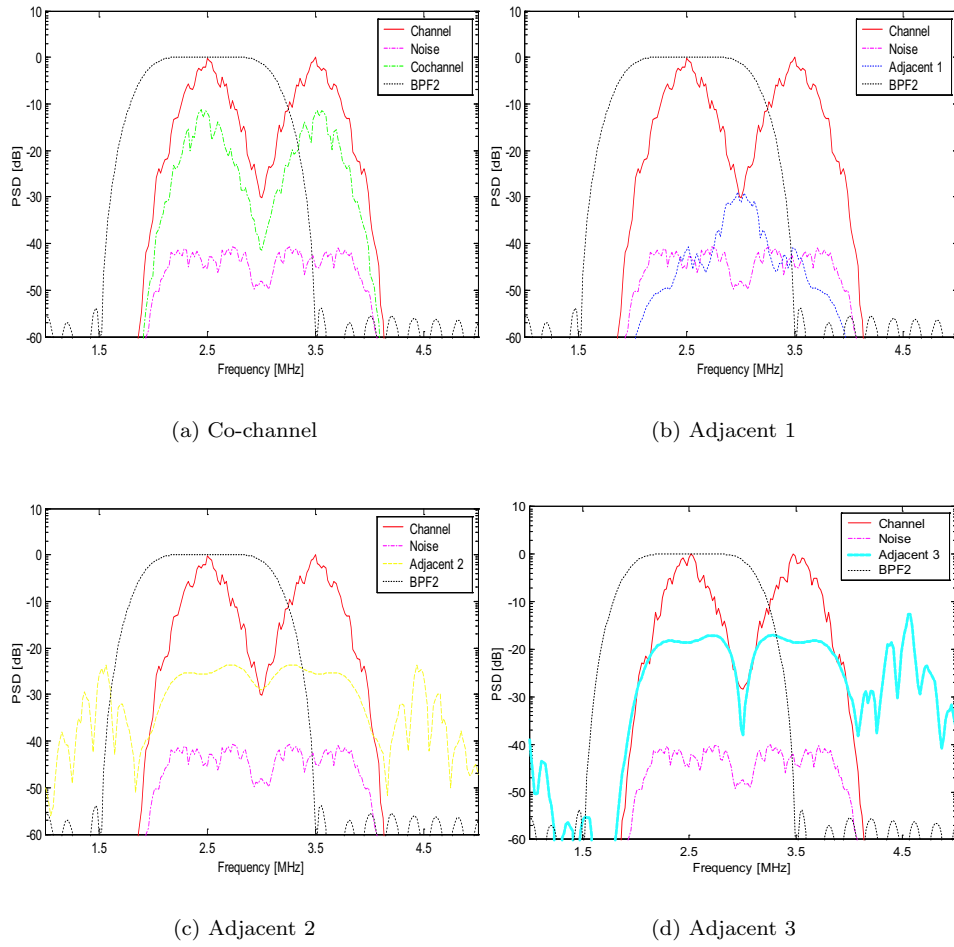


Figure 6.7: Transfer function of BPF2 filter and its incoming signal $g[n'']$

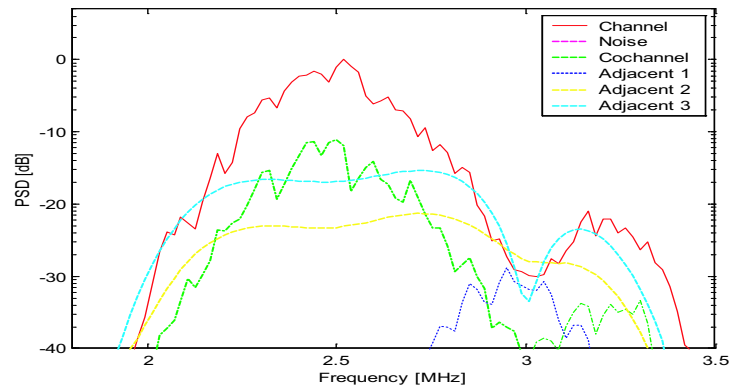


Figure 6.8: Demodulator input $h[n'']$

are equally closed or open.

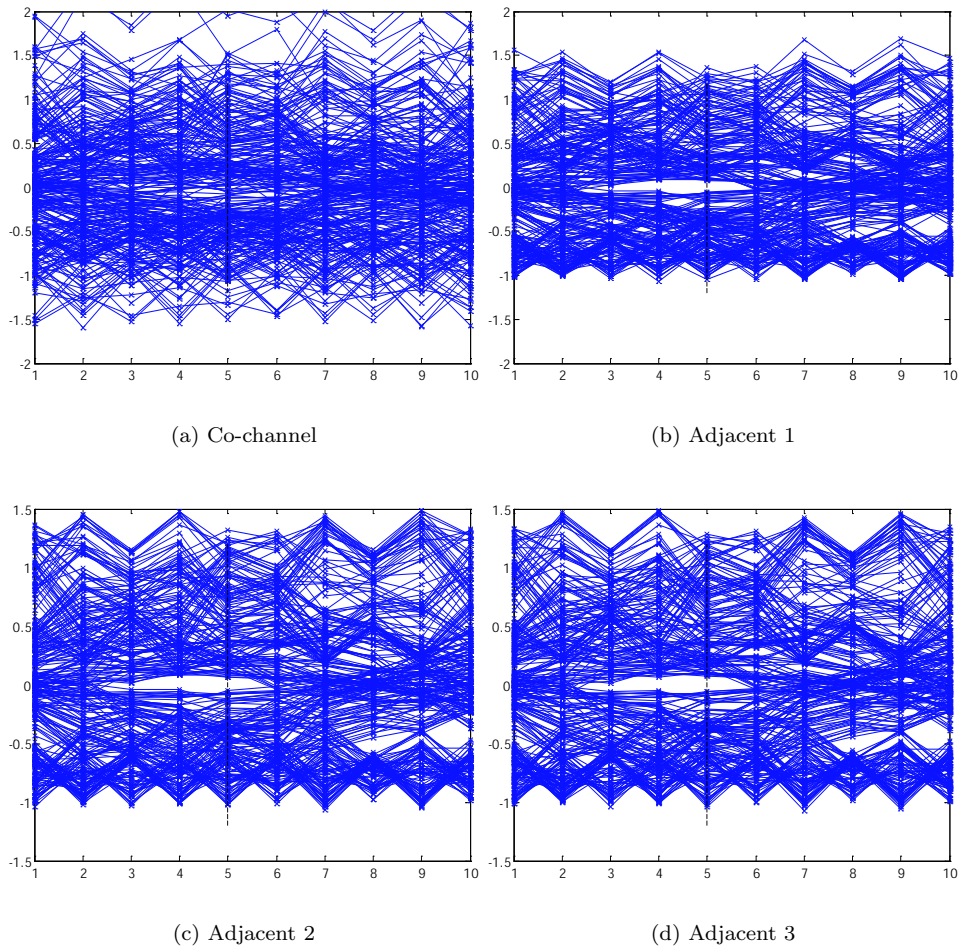


Figure 6.9: Eye diagrams of demodulated $h[n'']$ signals

6.3.6 BER calculations

The eye diagrams are obtained by repetitive plotting of one symbol period of the demodulated wave. This is done separately for each frame. Not all frames are alike, and it is likely that some bit sequences of some frames combined with some semi-coincidental circumstance cause bit errors that were not expected by analyzing eye diagrams. Thus, for more reliable comparison between channel selection systems, BER calculations are used. The bit error rates of the test signals after processing by the current system are all zero, except for the co-channel experiment which has $BER = 0.024$. This does not meet specifications and the filters must be redesigned. After several simulations, varying the transition band-width, pass-band ripple and filter order a system was found that meets specifications. This system will be described in the next section.

6.3.7 ASAP system 1 specification

Total filter operations for this FIR only approach is (values are taken from table 6.3.7): $1000 + 160 + 430 + 525 = 2115$ million MACs/s. This excludes the resources necessary for mixing and changing filter coefficients for BPF1. The latter will

Name	Hb	LPF	BPF1	BPF2
Type	FIR	FIR	FIR	FIR
Order	49	15	85	104
Method	Remez	Remez	Remez	Remez
$\Omega_{s,p}$ [rad/s]			[0.38 0.40]	[0.36 0.40]
$\Omega_{p,s}$ [rad/s]	[0.050.95]	[0.250.4]	[0.50 0.52]	[0.60 0.64]
δ_p [dB]	0.061	0.13	0.6	0.6
A_s [dB]	-	16	-23	-62
f_{filter} [MSPS]	80	80 (20)	20 (10)	10
MACs/s [$\cdot 10^6$]	2000(1000)	160	430	525

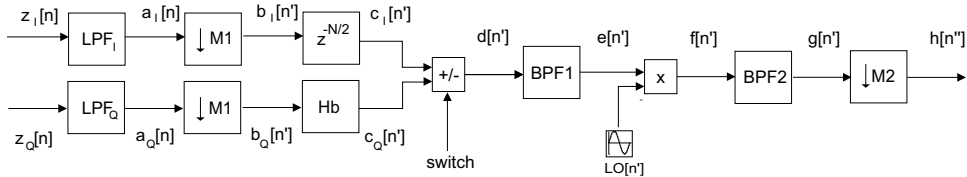
Table 6.4: Filter parameters **ASAP** system 1

require $(10 \cdot 86)/2 = 430$ memory spaces to store the (symmetric) coefficients. The Hilbert transformer has zero coefficients every other tap, so the MACS/s number can be halved. The Hilbert transformer is the largest performance bottleneck, but BPF1 and BPF2 are also very large (even if IIR filters would have been used). The aliasing due to the second decimation causes the adjacent 40 dB stronger interferer to alias into the f_{demod} region. Therefore, the stop-band attenuation requirement of the BPF1 filter are very strict and BPF2 cannot be used to "help". Thus, the second decimation prohibits benefitting from having two band-pass filters in the system. A second system is proposed that *does* take advantage of this situation.

6.4 ASAP system 2

6.4.1 Introduction

There are two issues that prevent the **ASAP** system 1 to perform well: the Hilbert transformer and the excessive aliasing due to the second decimation. These problems are both resolved in the second system, where a better trade-off between the BPF1 and BPF2 requirements becomes possible (see figure 6.10). The Hilbert transform is done *after* the first decimation and the A mixed FIR-IIR system will be proposed that performs significantly better than the first system.

Figure 6.10: Asap channel selection system 2 ($M1 = 4, M2 = 2$)

6.4.2 Moving the Hilbert bottle-neck

The Hb block is now placed *after* the low-pass filters. As a consequence, two (identical) LPFs are needed in the signal path. The response of the filter remains unchanged. Now, the Hb block is operating at a $M1$ times lower rate. This has the advantage of reducing the amount of filter operations, but also improves the pass-band response.

6.4.3 Reduce aliasing, improve BPF1/BPF2 cooperation

By delaying the second decimation until *after* BPF2, the required attenuation of adjacent channel interferers can be shared among two filters. This leads to a significant reduction in filter coefficients and compensates for the higher rate of BPF1. BPF1 is now the most critical filter with respect to performance. It is therefore a good approach to minimize BPF1 coefficients and compensate with BPF2. This can be illustrated by the following: two coefficients less used in BPF1 reduces the filter operations by $(2 \cdot 20 \cdot 10^6)/2 = 20$ MMAC/s (using the symmetric property) and memory usage by $1 \cdot 10 = 10$ registers (each channel has a different filter). Increasing BPF2 with 2 coefficients results in $((2 \cdot 20e6 \cdot 10^6)/2)/2 = 5$ MMAC/s and 1 extra register.

6.4.4 BPF1/BPF2 filter re-design

To design a BPF1 filter that will *just* allow the system to meet requirements, a closer look is taken into a so-called "critical" region. This is the region where all interferers "intersect" the selected Bluetooth channel. Figure 6.11 zooms in on the critical points of the BPF1 filter. α, β and γ show the interference floor of adjacent channels 3, 2 and 1 respectively. The challenge is to accept an increase of these levels that is as small as possible by choosing the optimal filter shape. The 45th order FIR filter response shown in figure 6.11 intercepts the interferers at points δ, ϵ and ζ . In this situation, the adjacent 3 channel is the strongest interferer. If a wider transition band is chosen, the ϵ intersection moves to the right. If f_ϵ approaches 5.3 MHz it moves beyond δ and this makes the adjacent 1 channel the strongest (resulting) interference. The gradient of adjacent channel 1 at point ϵ thus imposes constraints on the BPF1 filter. If a wider transition band is chosen, this is the first test that will fail. Adjacent 3 becomes a problem after mixing, as the stop-band attenuation of BPF1 is poor (in an effort to save coefficients). BER experiments have lead to a FIR BPF1 implementation of order $N = 45$. The trade-offs that have been made are listed in the following section.

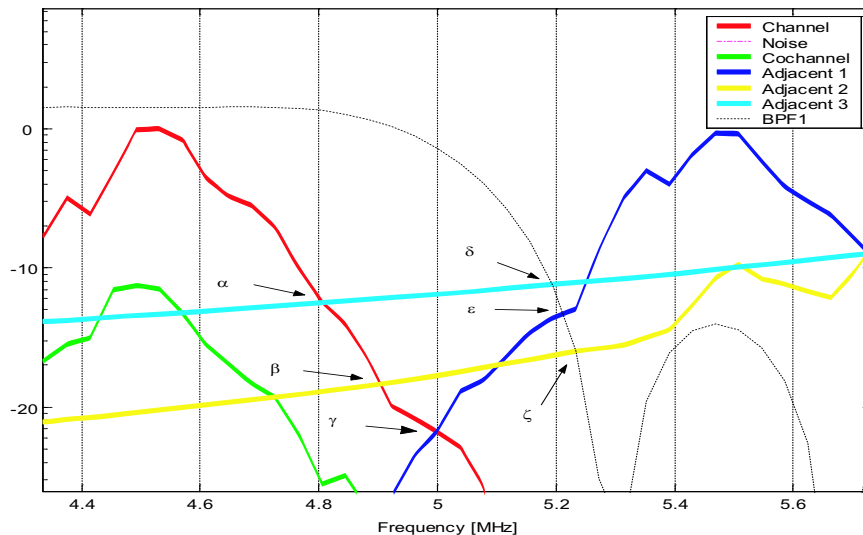


Figure 6.11: BPF1 response and incoming signals, model 2

Name	LPF (2x)	Hb	BPF1	BPF2
Type	FIR	FIR	FIR	FIR
Order	15	49	50	45
Method	Remez	Remez	Remez	Hamming
$\omega_{s,p}$ [rad/s]			[0.38 0.40]	[0.185]
$\omega_{p,s}$ [rad/s]	[0.250.5]	[0.10.9]	[0.50 0.52]	[0.315]
δ_p [dB]	0.13	0.061	0.7	0
A_s [dB]	21	-	-17	-62
f_{filter} [MSPS]	80 (20)	20	20	(20) 10
MACs/s [$\cdot 10^6$]	160	250	500	225

Table 6.5: Filter parameters **ASAP** system 2, FIR-only

6.4.5 Sensitivities and trade-offs

The sensitivities and trade-offs involving the reduction of filter operations while maintaining specified bit error rates are:

Filter order Higher order filters reduce the BER of the adjacent channel experiments (BER tests 2,3 and 4). On the other hand, it reduces the performance of the co-channel experiment (BER test 1). The eye diagram shows a direct inverse relation between the filter order and the "open-ness" of the eye.

Filter bandwidth The width of the flat pass-band must be chosen as wide as possible, without allowing too much adjacent channel interference. The demodulator has a large dependency on the outer rims of the channel spectrum. The obvious solution to this problem is a very steep filter, but this is only feasible for IIR, which introduce the largest phase non-linearities in that critical region. Thus, the trade-offs are made in the transition bands.

Transition bands The critical points of the filter design are the intersections with the adjacent channels. The optimal balance of the conflicting requirements imposed by the 4 tests lie in the distribution of the interferences. In other words: the least amount of processing power is used when the eye diagrams of all 4 BER tests are equally closed.

6.4.6 ASAP system 2 specifications

The currently proposed system based on the **ASAP** model can be implemented by using FIR-only or mixed FIR-IIR filter systems. The performance figures for the FIR-only system are listed in table 6.5. The bit error rate achieved was $1.16 \cdot 10^{-4}$ for adjacent 3 and zero for the rest. The performance figures for the IIR replacements for BPF1 and BPF2 are listed in table 6.6. The bit error rates achieved are $1.16 \cdot 10^{-4}$ for co-channel, $5.82 \cdot 10^{-5}$ for adjacent 1 and zero for adjacent 2 and 3. The Chebyshev Type II design method was used for BPF1, as it has similar (and in this case even better) linear phase response characteristics than Butterworth filters. These were not studied in chapter 4, section 4.4 but have been tested because of their moderate non-linear phase response. The Chebyshev Type II filter allows ripples in the stop-band, and this can be used to reduce the pass-band width. Overall, the Chebyshev filter behaves more like the Remez (BPF1) filter in the FIR-only model and the Butterworth filter is more similar to the Hamming window filter (BPF2). The performance figure of the FIR-only system is $PF_{FIR-only} = 160 + 250 + 500 + 225 = 1135$ MMAC/s (refer to table 6.5). By replacing the FIR band-pass filters for IIR alternatives this becomes $PF_{FIR-IIR} = 160 + 250 + 200 + 140 = 750$ MMAC/s (refer to table ??). The negative side-effects of the changes made to the system are

Name	<i>BPF1</i>	<i>BPF2</i>
Type	IIR	IIR
Order	4 (5, 5)	6 (7, 7)
Method	Chebyshev Type II	Butterworth
$\Omega_{s,p}$ [rad/s]	[0.375, 0.390]	0.2
$\Omega_{p,s}$ [rad/s]	[0.505, 0.525]	0.3
δ_p [dB]	0	0
A_s [dB]	30	20 (at [0.16, 0.37])
f_{filter} [MSPS]	20	20 (10)
Mac/s [$\cdot 10^6$)]	200	140

Table 6.6: Filter parameters for IIR BPF1 and BPF2 (**ASAP** system 2)

that the number of required oscillator frequencies for the digital mixer have risen from 2 to 7 and the operating frequency of the local oscillator has doubled. However the reduction in filter operations and coefficients for reloading is a big advantage.

6.5 ALAP system

The ALAP model has been briefly simulated because BER tests were unsuccessful for filters under $N = 150$. Taking into account that 3 or 4 times 151 coefficients must be multiplied with 20 million incoming samples this system will need almost a GMAC/s to operate. If a future demodulator would require complex inputs, it may be worth it to research this model further. In this work however, this was not done.

6.6 Conclusions

Based on the systems that were researched the initial assumptions that a complex system is likely to require more processing proved valid. The *real* design was implemented and improved and is proposed as the optimal solution for the current requirements with respect to the derived performance figure. The PF of this system is 750 MMAC/s for a mixed FIR-IIR implementation and 1135 MMAC/s for FIR-only.

Conclusions and Recommendations

7.1 Conclusions (Summary)

Based on a derivation of Bluetooth and HiperLAN/2 channel selection requirements, filter specifications and overall system design options were formulated for the digital channel-selection system. Due to the nature of the project in which this work was done, several parameters were unknown at the start of my MSc-work. This called for an approach of scenario's and broad system perspective.

After researching different filter types and structures a provisory channel selection system for *HiperLAN/2* was proposed. The proposed HiperLAN/2 digital channel-selection system receives complex signals from the analog front-end provides the wanted channel to the demodulator as a complex channel. The system consists of two (real) identical low-pass anti-alias filters followed by a decimator. After decimation by 2, a pair of identical (real) low-pass channel selection filters are used to provide sufficient attenuation of the adjacent interferences. Due to late availability of a demodulator, this system was not further researched and no channel-selection tests or BER tests were executed.

For *Bluetooth* digital channel-selection, the input signals are complex, while the output signal, the input for the demodulator was required to be real. This lead to two main scenario's that were researched. The first was based on converting the complex signals to real as soon as possible, leading to the so-called **ASAP** system. The second scenario used the opposite approach and lead to the so-called as late as possible **ALAP**-system, in which mixed real and complex filtering could be done. The initial assumptions that a (partly) complex system is likely to require more processing proved valid. The *real* design was implemented and improved and is proposed as the optimal solution for the current requirements with respect to the derived performance figure (MMAC/s).

The original **ASAP2** design in which only FIR filters are used (see section 6.4.6, table), needs 1135 MMAC/s for channel selection. In it, the incoming quadrature signals are low-pass filtered by a pair of (real) FIR filters, implemented in polyphase. Then, they are converted to a bandpass signal by using a FIR Hilbert transformer and adder. Changing the sign bit of the adder is the first stage of channel selection. Band-pass filtering is done by a 50th order Remez equiripple filter and a 45th order Hamming windows filter. To reduce filter operations the usage if IIR filters was researched, leading to a **ASAP2** mixed FIR-IIR system. The FIR-only design is maintained so it can be used in case IIR filters are not suitable for implementation.

The system that performed best, the **ASAP2** mixed FIR-IIR system (see section

6.4.6, tables with BPF1 and BPF2 taken from 6.6) uses 750 MMAC/s for channel selection. The signals are band-pass filtering by a *variable* 4th order Chebyshev Type II IIR filter. The filter is variable in the sense that filter coefficients must be updated every time the Bluetooth signal hops to another frequency. Then the filtered signal is mixed to the required frequency for demodulation. After a second band-pass filter (6th order Butterworth IIR filter) the signal is decimated again and ready for demodulation.

Both ASAP systems meet BER requirements as specified in the Bluetooth documentation. Thus, the currently proposed models use real filters and offers good channel selection and performance for the currently proposed demodulator.

7.2 Recommendations

There are six recommendations I would like to make:

- Starting with the analog front-end and the ADC. It is quite possible that due to the analog filtering and low signal distortion by the ADC, the digital LPF can be omitted entirely.
- Furthermore, the demodulator requires a real input signal, but internally mixes it to baseband, applies low-pass filtering and then demodulates. In a more optimal design, the channel selection system converts the incoming signal to baseband in stead of a second IF. In this situation, the total performance figures are likely to favor quadrature channel selection, as opposed to the currently proposed real system.
- The current approach was based mainly on simulations. An interesting study would be a formal analysis of the complete system, including demodulation. Based on the relations found between the filters and the sensitivity of the frequency demodulation a more exact solution may be found for the filter designs.
- Automatic Gain Gontrol. The current simulation model has fixed gains, resulting in poor BER performance if the input signal becomes small. The AGC implementation should be done in cooperation with the demodulator design(er). Automatic gain and gain adjustment for quantization may also be jointly researched, as the operations are similar.
- Fixed Point Analysis. Although the current system was designed with fixed point implementation in mind, it was not explicitly researched. The used filter responses are nearly identical with 16 bit fixed point quantization. For IIR filters, second order sections are needed to prevent instability.
- Filters. The IIR filter family also includes Bessel filters, which deserve a closer look. They are reported to have the best linear phase characteristics and group delay response.

A

Quadrature signals

A.1 In-phase and Quadrature signals

A real (band limited) signal $s(t)$ is mixed with two local oscillators, represented by $\cos(2\pi f_{lo}t)$ (in the I path) and $\sin(2\pi f_{lo}t)$ (in the Q path). Mathematically, this can be represented by:

$$I(t) = s(t) \cdot \cos(2\pi f_{lo}t) = \frac{s(t)}{2} \cdot e^{j2\pi f_{lo}t} + \frac{s(t)}{2} \cdot e^{-j2\pi f_{lo}t}$$

and

$$Q(t) = s(t) \cdot \sin(2\pi f_{lo}t) = j \cdot \left(\frac{s(t)}{2} \cdot e^{j2\pi f_{lo}t} - \frac{s(t)}{2} \cdot e^{-j2\pi f_{lo}t} \right)$$

Multiplying Q by j^{-1} yields (bearing in mind that $j^2 = -1$):

$$j \cdot Q(t) = -\frac{s(t)}{2} \cdot e^{j2\pi f_{lo}t} + \frac{s(t)}{2} \cdot e^{-j2\pi f_{lo}t}$$

Addition of $I(t)$ and $jQ(t)$ yields:

$$s(t) \cdot \left(\frac{1}{2} \cdot e^{j2\pi f_{lo}t} - \frac{1}{2} \cdot e^{j2\pi f_{lo}t} + \frac{1}{2} \cdot e^{-j2\pi f_{lo}t} + \frac{1}{2} \cdot e^{-j2\pi f_{lo}t} \right)$$

The first two terms inside the brackets cancel each other out, the last two terms add up:

$$I + j \cdot Q(t) = s(t) \cdot e^{-j2\pi f_{lo}t}$$

Subtracting I and jQ results in the opposite (positive) spectrum:

$$I - j \cdot Q(t) = s(t) \cdot e^{j2\pi f_{lo}t}$$

A.2 Quadrature down conversion of signal chunks

The complex mix operation discussed in section 3.2 also applies to band-pass signals. The spectra of $x(t)$ before and after quadrature down conversion are shown in figure A.1.

¹ $\exp \frac{\pi}{2} = \cos(\frac{\pi}{2}) + j \cdot \sin(\frac{\pi}{2}) = 0 + j \cdot 1 = j$ so we are changing the phase 90 degrees

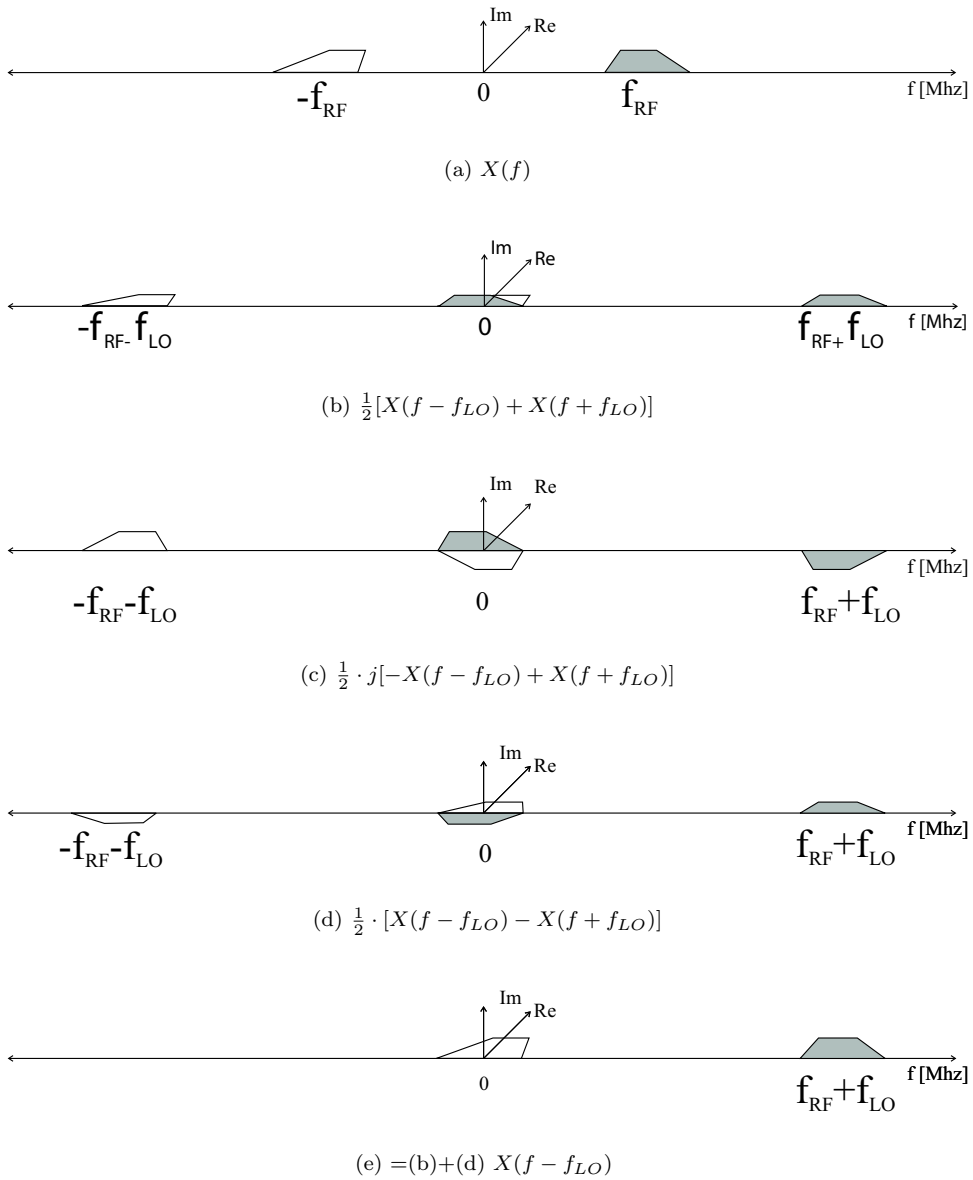


Figure A.1: Spectra of even (I, Q) signal paths

B

The Hilbert transform

A Hilbert transform can be implemented by a FIR or IIR filter [14]. Then, it is defined as an all-pass filter with an (ideal) transfer function given by [14],[13],[21]:

$$\begin{aligned} H(f) &= -j \text{ for } f \geq 0 \\ H(f) &= j \text{ for } f < 0 \end{aligned} \tag{B.1}$$

The impulse response of a FIR Hilbert transformer is shown in figure B.1. The left half of the coefficients are the negative image of the positive half. Every other coefficient is zero, reducing filter operations. The error caused by finite word and filter lengths is in the output signal amplitude, rather than phase. The pass-band

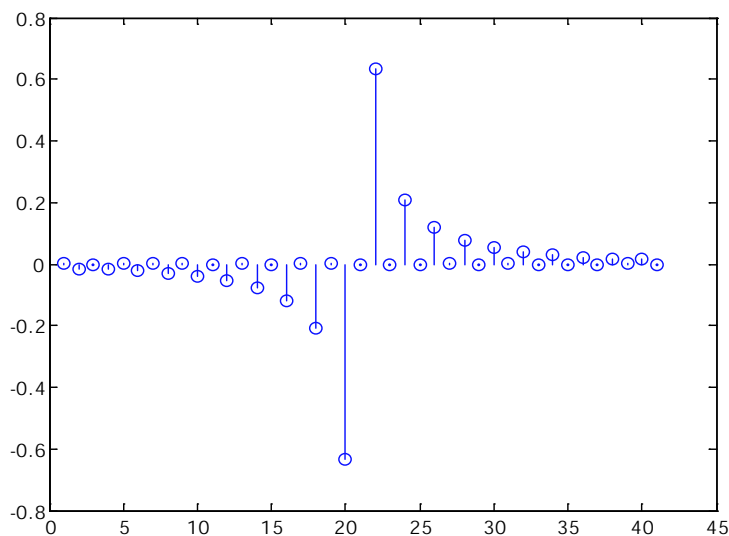


Figure B.1: FIR Hilbert transformer ($N = 40$) impulse response

width, ripple and overshoot characteristics are dependent on the number of taps and window used to truncate the Fourier series. The rectangular windows produces the largest pass-band and largest overshoot (Gibbs' phenomenon, refer to section 4.2.2).

B.1 Practical usage for channel selection

Recall figure A.1 on page 65. By taking the Hilbert transform of $\tilde{z}_Q(n)$ and adding/subtracting the result to/from $\tilde{z}_I(n)$, the lower/upper half of the complex $\tilde{Z}[f]$ spectrum is selected. Furthermore, the resulting signal is real and its frequency spectrum thus symmetrical around 0. Graphically, it is similar to figure A.1(c), but now the positive frequencies are rotated clockwise. To see what happens, assume that the signal chunk in figures 3.3 and A.1 represent 10 Bluetooth channels. After low-pass filtering and AD conversion, the $z_I(n)$ and $z_Q(n)$ signals can be represented by figures B.2(a) and (b). After (ideal) Hilbert transformation, $\text{Hilbert}(z_Q(n)) = z_{QH}(n)$ looks like (c). Now $z_I(n)$ and $\text{Hilbert}(z_Q(n))$ can be added (or subtracted), and a real signal is formed. This way, a (baseband) signal with uneven spectrum is converted to a real signal with an even spectrum. In the process, half of the spectrum is lost. The sign of the final adder determines which half. In literature this method is called upper/lower sideband selection. A general purpose sub-block to be used in the system, based on this principle is depicted in figure B.3.

B.2 Upper/lower sideband rejection

This signal consists of either the positive or negative half of the baseband spectrum (including it's image, see figure B.2(d)). The degree of sideband rejection depends on the pass-band ripple and thus the amount of filter coefficients. To exactly cancel out a strong interferer by adding a delayed copy of itself requires a maximally flat magnitude response. For Bluetooth, the worst-case would be a +40 dB stronger interferer at $-fc$, requiring over $40 + 21 = 61$ dB of rejection. This results in a maximum allowable ripple of (using eq. 4.4):

$$\delta_p = 10^{\frac{-61}{20}} \approx 8.9 \cdot 10^{-4}$$

The transition bandwidth (as specified in 2.4) for a filter frequency of 20 Msps is equal to:

$$\Delta_f = \frac{f_p}{f_{filter}} = \frac{0.162}{20} \approx 8.1 \cdot 10^{-3}$$

A FIR implementation of a Hilbert transformer using a Kaiser window, the required order the filter becomes [14]:

$$N \approx \frac{-0.61 \cdot \log_{10}(\delta_p)}{\Delta_f} \approx 224 \tag{B.2}$$

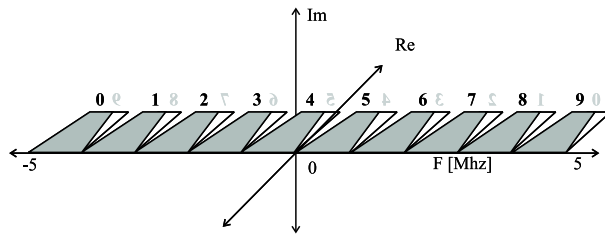
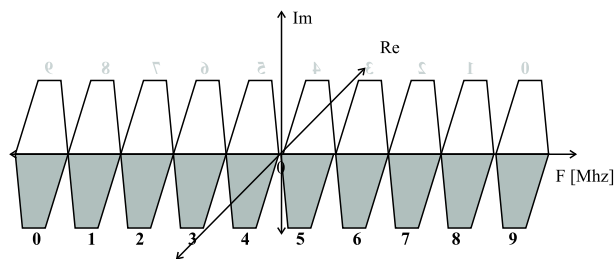
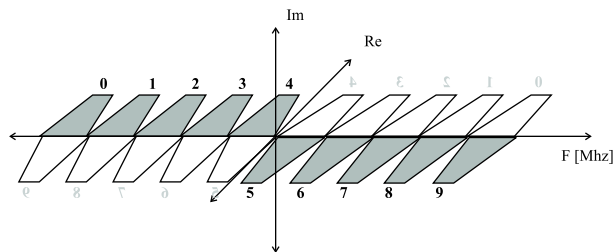
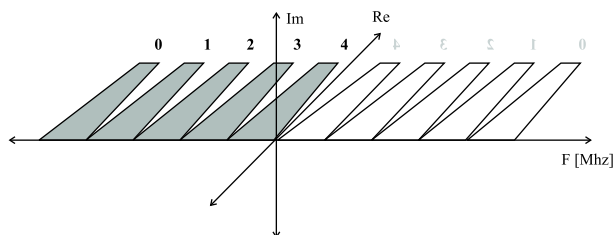
(a) $Z_I(f)$ (b) $Z_Q(f)$ (c) $Z_{QH}(f)$ (d) $Z_I + Z_{QH}(f)$

Figure B.2: Create real USB/LSB signal

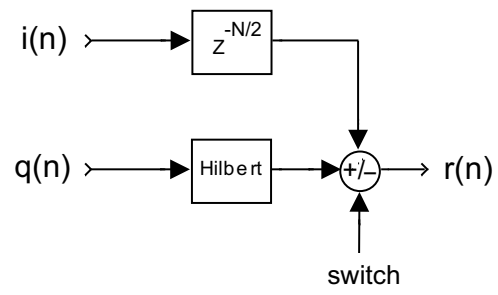


Figure B.3: USB/LSB selection using the Hilbert transform

C

Noble identities

The scaling (a_1) and (a_2) of signals and the decimation (M) in the different branches of the digital filter structures is independent of the sampling rate [12]. Therefore, the structures of C.1(a) and (b) are equivalent. A delay of M sample periods before a down sampler, is equivalent to a delay of 1 sample period after the down sampler. This leads to the second identity shown in figures C.1(c) and (d). A useful consequence is the identity shown in C.1(e) and (f).

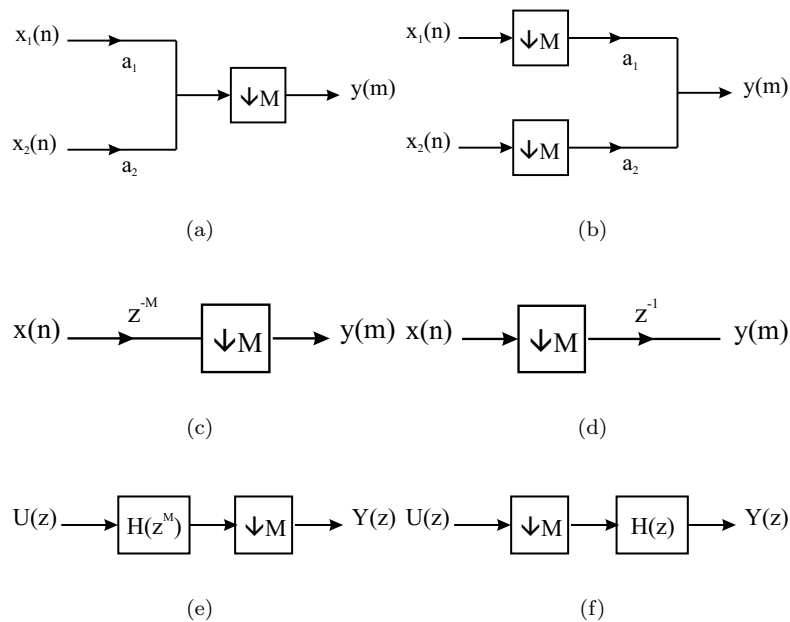


Figure C.1: Noble identities

This is an interesting property of digital signal processing and by this switching function a hopping Bluetooth channel can be "followed" more easily without reloading filter coefficients.

Bibliography

- 1 A. Antoniou. *Digital filters: Analysis, design, and applications*. McGraw-Hill, 1993.
- 2 Conexant. On the direct conversion transceiver. <http://www.conexant.com>, 7 2001. Application note.
- 3 M. P. Donadio. Cic filter introduction, 7 2000. For free publication by Iowegian.
- 4 D. Grover et al. *Digital Signal Processing and the Microcontroller*. Prentice Hall, 8 1998.
- 5 F.W. Hoeksema et al. Evaluation of hiperlan/2 channel selection filters. SDR project R007v01 2, August 2002.
- 6 F.W. Hoeksema et al. Realization and testing of the software radio based bluetooth - hiperlan/2 demonstrator, 7 2002.
- 7 F.W. Hoeksema et al. Specification for digital channel selection filters in a bluetooth capable hiperlan/2 receiver. Conference Paper 1, 2 2002.
- 8 J.G. Proakis et al. *Digital Signal Processing*. Maxwell Macmillan, 1993.
- 9 L. Hanso et al. *Single- and Multi-carrier Quadrature Amplitude Modulation*. John Wiley & Sons, 2000.
- 10 R. Schiphorst et al. Bluetooth demodulation algorithms and their performance. Paper 1, 2 2002.
- 11 V.J. Arkesteijn et al. Physical layer functions of a software radio based bluetooth - hiperlan demonstrator. Project Internal TES.5177/ALL/MA/PI/D/002/01, University of Twente, 7 2001.
- 12 N.J. Fliege. *Multirate Digital Signal Processing*. John Wiley & Sons, 1994.
- 13 M.E. Frerking. *Digital signal processing in communication systems*. Chapman & Hall, 1993.
- 14 S.L. Hahn. *Hilbert transforms in signal processing*. 1996.
- 15 L.W. Couch II. *Digital and Analog Communication Systems*. Prentice Hall, 2001.
- 16 T. Kaitz. Performance aspects of ofdm phy proposal. Technical report, March 2001. IEEE 802.16 Broadband Wireless Access Working Group <http://ieee802.org/16/>.
- 17 K.D. Kammeyer. *Nachrichtenübertragung*. B.G. Teubner, 1996.
- 18 R. G. Lyons. *Understanding digital signal processing*, 1996.

- 19 U. Meyer-Baese. *Digital Signal Processing with Field Programmable Gate Arrays*. Springer, 2001.
- 20 PACT. Fir filter for complex integers on the xpu128. <http://www.pactcorp.com>, 9 2000. Application Note.
- 21 P.P. Vaidyanathan. *Multirate Systems and filter banks*. Prentice Hall, 1993.
- 22 L.F.W. van Hoesel. Design and implementation of hiperlan/2 physical layer models for simulation purposes. Masters thesis, August 2002.
- 23 Various. Specification of the bluetooth system. Specification 1.1, 2 2001.
- 24 Xilinx. Cascaded integrator-comb (cic) filter. <http://www.xilinx.com>, 10 2001. Product specification.